Kent Academic Repository

Full text document (pdf)

Citation for published version

Yigal, Leiba and Dayan, Elad and Yaron, Fein and Steeg, Matthias and Stöhr, Andreas and Inoue, Toshiyuki and Murata, Hiroshi and Nair, Manish and Gomes, Nathan J. and Yonemoto, Naruto and Szcz sny, Micha and koscieszа, Micha (2018) Radio technologies for 5G using Advanced Photonic Infrastructure for Dense user environments - D321 Report on Beam Steerable Directive

DOI

Link to record in KAR

https://kar.kent.ac.uk/71481/

Document Version

Publisher pdf

Copyright & reuse
Content in the Kent Academic Repository is made available for research purposes. Unless otherwise stated all content is protected by copyright and in the absence of an open licence (eg Creative Commons), permissions for further reuse of content should be sought from the publisher, author or other copyright holder.

Versions of research
The version in the Kent Academic Repository may differ from the final published version.
Users are advised to check **http://kar.kent.ac.uk** for the status of the paper. **Users should always cite the published version of record.**

Enquiries
For any further enquiries regarding the licence status of this document, please contact:
researchsupport@kent.ac.uk

If you believe this document infringes copyright then please contact the KAR admin team with the take-down information provided at **http://kar.kent.ac.uk/contact.html**

KAR Kent Academic Repository

University of Kent

RAPID5G

Radio technologies for 5G
using Advanced Photonic Infrastructure
for Dense user environments

Project Coordinators:

Andreas Stöhr
University of Duisburg-Essen
Germany

Hiroshi Murata
Osaka University
Japan

European Horizon 2020 Programme Project:
RAPID, ICT- 643297, 1. October 2014 – 30. September 2017

Report on beam steerable directive antennas

Deliverable / Milestone n°: D321
Deliverable / Milestone type: Deliverable
Dissemination level: Confidential
Report preparation date: 31 October 2016
Authors:

	Leiba Yigal, Elad Dayan, Yaron Fein	Siklu Communication
	Matthias Steeg, Andreas Stöhr	Universität Duisburg-Essen
	Toshiyuki Inoue, Hiroshi Murata	Osaka University
	Manish Nair, Nathan Gomes	University of Kent
	Naruto Yonemoto	ENRI
	Michał Szczęsny, Michał koscieszа	Exatel

Abstract:

This deliverable reports the beam-steering architecture implementation in the RAPID 5G. Various beam-steering antenna methods are reviewed and several are chosen for implementation. The construction of the antenna for each of the chosen methods and measurement results for the constructed prototypes are reported.

Project funded by the European Commission and the National Institute of Information and Communications Technology within the "ICT - Information and Communication Technologies" Programme under EU-Japan Research and Development Cooperation in Net Futures - EUJ 3 – 2014: Access networks for densely located users

Table of Contents

© RAPID5G Consortium

1 Executive Summary

This deliverable reports about the beam-steering architecture implementation in the RAPID 5G architecture. The position of the beam-steerable antennas in the architecture is described and various beam-steering antenna methods are reviewed. Some of the methods reviewed have been chosen for implementation. The construction of the antenna for each of the methods selected is described. The selected methods include travelling wave and electro-optical beam steering antennas for 1D beam steering required for the 5G hot spot (download kiosk) application and the beam switching and beam-steering antennas for the 2D beam steering required for the heterogeneous 3G/4G/5G demo in the shopping mall. Each of these antennas has different performance capabilities and the performances of these various antennas are measured. The measurement results are reported and compared with the desired characteristics specified in the RAPID subsystem and component specifications deliverable ([3]).

© RAPID5G Consortium

2 Definitions and abbreviations

2.1 Terminology definition

AAE: Array antenna electrode
AWGN: Additive white Gaussian noise
BBU: Base band unit
BER: Bit error rate
BW: Bandwidth
DC: Direct current
EO: Electro optic
EVM: Error vector magnitude
FEC: Forward error correction
IC: Integrated circuit
IF: Intermediate frequency
IFFT: Inverse Fourier transform
LO: local oscillator
LTCC: Low temperature co-fired ceramic
LTE: Long term evolution
LWA: Leaky waveguide antenna
MEMS: Micro electro mechanical sensor
MIMO: Multiple input multiple output
MMW: Millimetre wave
NF: Noise figure
OFDM: Orthogonal frequency division multiplexing
PA: Power amplifier
P2P: Point-to-point
P2MP: point-to-multipoint
PCB: Printed circuit board
PLL: Phase locked loop
QAM: Quadrature Amplitude Modulation
RAU: Remote access unit
RF: Radio frequency
RFIC: Radio frequency integrated circuit
SDM: Space division multiplexing
SIW: Substrate integrated waveguide
SNR: signal-to-noise ratio
VNA: vector network analyzer

© RAPID5G Consortium

3 Beam-steerable antennas in RAPID

The beam-steerable directional antennas are an essential part of the wireless link when operating at mm-wave frequencies. The reason for that is that the coverage footprint achievable at broadband mm-wave channel is simply too small when deploying omni-directional antenna, due to the free-space loss. This section describes the position of the mm-wave transceiver and its beam-steering antenna in the overall RAPID system. In order to do that, this section describes the overall system for the shopping mall scenario and attempt to place the mm-wave transceiver and beam steering antenna in this context.
As outlined in D211 ([1]), one of the key aims of the shopping mall field trial is to demonstrate mobility in a heterogonous network environment by enabling handovers between 3G/LTE, 802.11 and a RAPID-5G 60 GHz cell. The following figure illustrates the functionality of the shopping mall field trial (see also D211).

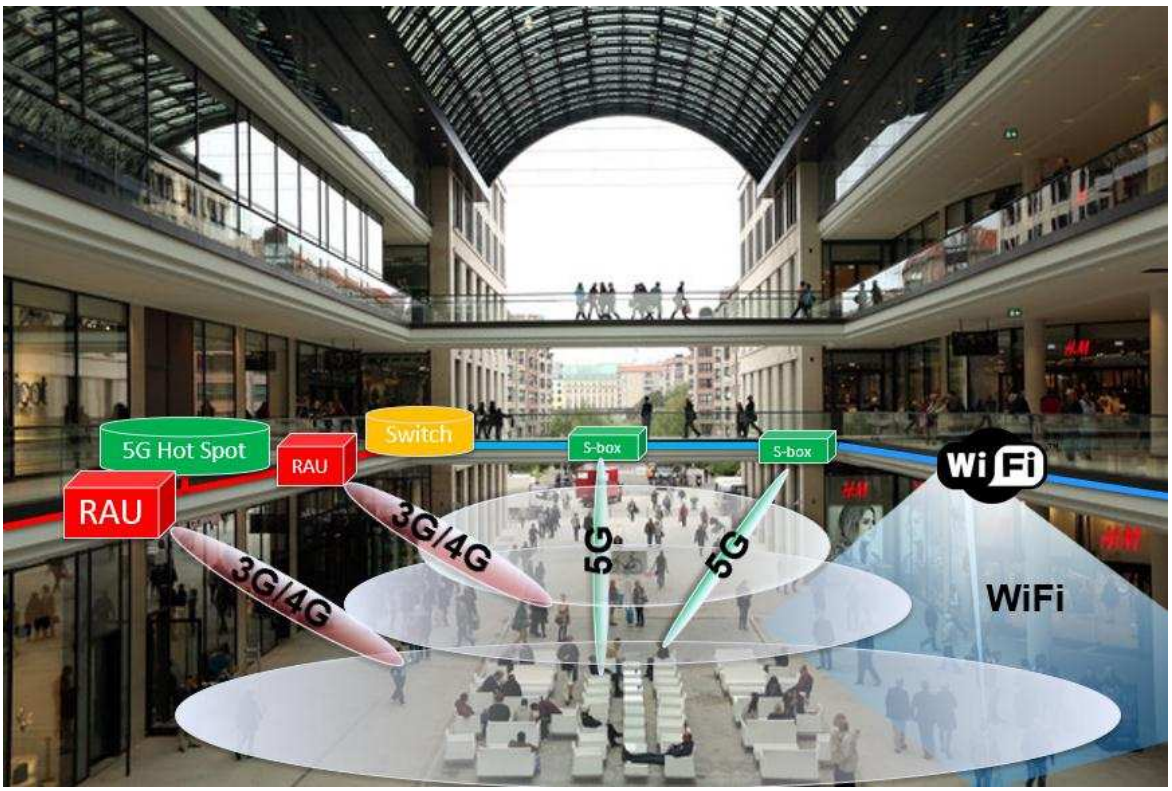

Figure 1: Illustration of the shopping mall field trial for demonstrating switchover in a heterogeneous network (WiFi & 60 GHz) and a 60 GHz hot spot

The system architecture for the shopping mall use case covering the heterogeneous 3G/4G/5G network architecture and the 60 GHz hot spot (kiosk download) use case has already been reported in D222. The following figure illustrates the system architecture.

© RAPID5G Consortium

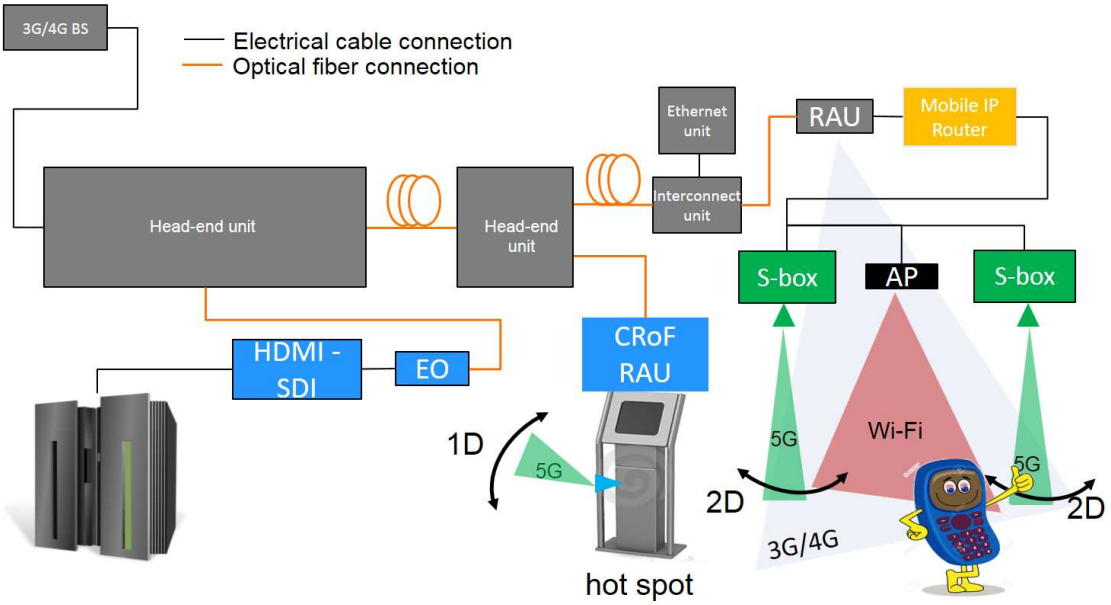

Figure 2: Shopping mall field trial for demonstrating a 60 GHz hot spot (kiosk download) and a heterogeneous network (WiFi & 60 GHz)

As illustrated in the figure, for the 60 GHz hot spot scenario the mobility of the user standing close to the download kiosk only requires 1D beam steering in the horizontal domain whereas the 60 GHz cell requires full 2D beam steering. For the 1D hot spot use case, low-cost 60 GHz travelling-wave antennas are considered.

The system architecture for demonstrating the switchover in the heterogeneous network (WiFi & 60 GHz) has been already described in D421 and it is shown for reference in the below figure.

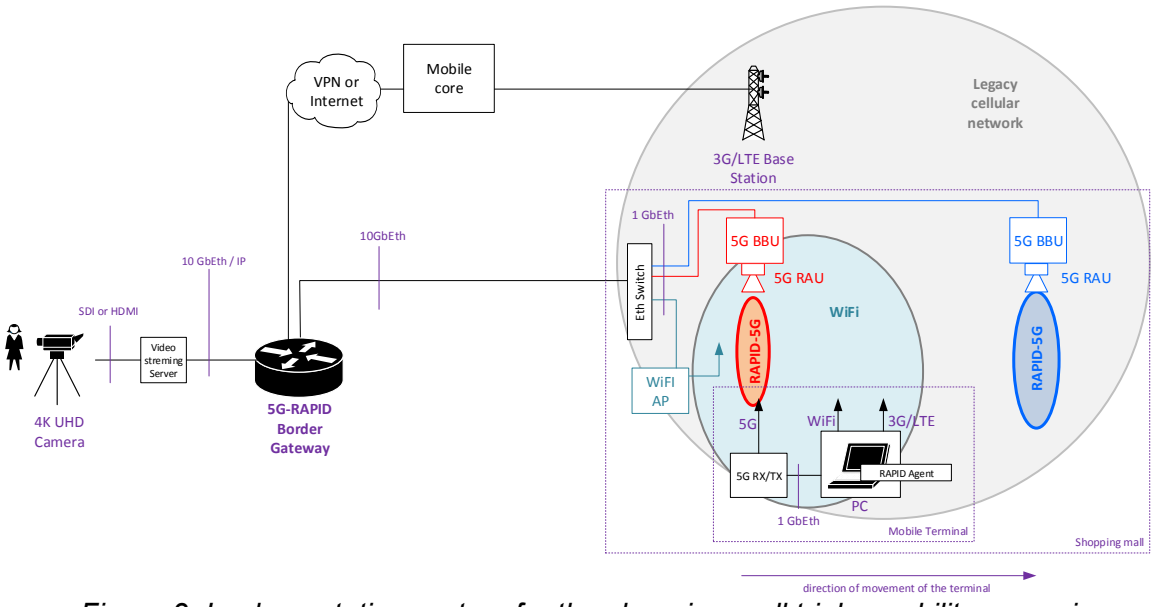

Figure 3: Implementation system for the shopping mall trial – mobility scenario

© RAPID5G Consortium

As can be seen, the 5G-RAPID border gateway is to be connected to the RAPID 5G RAU via a Gigabit Ethernet connection. Details of that connection are shown in the figure below. The border switch with a 10 GbE connection will be connected to the RAPID baseband unit (BBU) via a commercially available Ethernet switch. On the physical layer, the RAPID BBU is a media converter between 1 GbE and analog baseband I/Q signals. It is thus expected that each transceiver can handle at least 1 Gb/s data. For the 2D beam steering required for the 60 GHz cell, lens-assisted beam switched and beam steering antennas are considered.

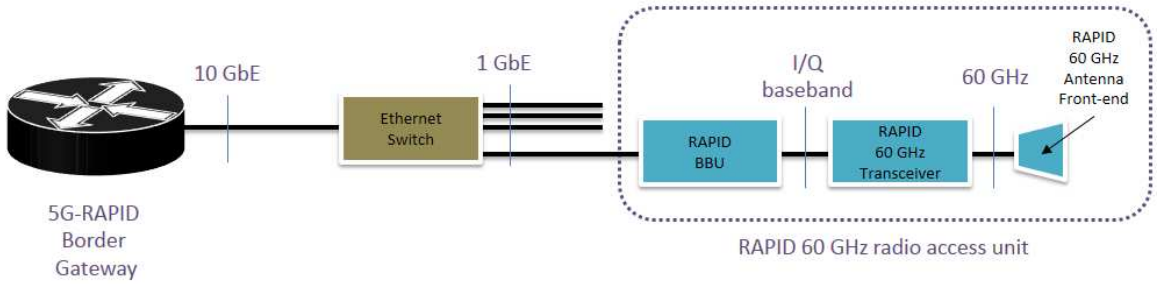

Figure 4: Implementation system connecting the RAPID5G radio access unit (RAU) to the 5G border gateway via an Ethernet connection

This deliverable D321 will report on the technological development of the RAPID 5G beam-steering travelling-wave antennas for the 1D hot spot scenario and the lens-assisted beam switched and beam steering antennas for the 2D 60 GHz cell scenario. The electro-optical antennas for the stadium use case will be reported as planned in D322.

© RAPID5G Consortium

4 Antenna specifications

The 60GHz spectrum is as attractive operation band to support the throughput and density requirements of a 5G cellular system due to the large quantities of spectrum it can offer as well as its high absorption of the radio signals. The high radio signal absorption is due to Oxygen molecules in the air, and it guarantees fast decay of interference. The challenge associated with operation at mm-wave frequencies from the antenna perspective is that use of omni-directional antennas offers very limited coverage footprint. To demonstrate this limitation, assume the following operation parameters taken from D221 ([3]),

Parameter	Specification	Comments
Band of operation	57-64GHz	
BW	1.9GHz	
Max. linear TX power	10dBm	P1dB figure
RX NF	5dB	Noise floor added by the RF chip
Operation desired SNR	13dB	Defines the desired C/N level to maintain desired user throughput and spectral efficiency of ~2bits/sec/Hz (e.g. 16QAM at FEC rate 1/2). Factors in a reasonable implementation loss

Table 1: PHY and radio operating parameters

The system gain can be calculated by using the equation below,

$$G_{SYS\_dB} = G_{ANT\_TX} + G_{ANT\_RX} + P_{TX} - 10 \cdot \log_{10} kTB - SNR_{TH}$$

Where the thermal noise floor given by $10 \cdot \log_{10} kT$ is -174dBm/Hz which yields a system sensitivity of -63dBm for the desired mode of operation. Since we assume omni-directional antennas with 0dBi gain, the only additional contribution to the system gain comes from the transmission power, resulting in G_{SYS_dB}=73dB.

The free-space path loss formula is $A_{dB} = 20 \cdot \log_{10} \frac{4\pi d}{\lambda}$ where the wavelength λ at 60GHz is roughly 5mm. Assuming the free-space loss is equal to the system gain, we get a propagation distance d of roughly 1.8m, which clearly is too short for decent cellular coverage.

The calculation above demonstrates why beam-steering antennas are a must when attempting to design a non-directional system operating at 60GHz mm-wave frequency. The antenna specifications from D221 are

Parameter	Specification
Gain	25dBi
Scan angle	90°
Operation bandwidth	57-64GHz
Coherence bandwidth	2.5GHz

Table 2: Beam-steering antenna specification

When using this specification in the system gain formula above, the system gain increases by 50dB (as the antenna is counted twice, once for TX and once for RX) to 123dB. Going back to the free-space loss formula and substituting the new system gain, we now get a coverage distance higher than 500m. This number is of-course inaccurate, as the free-space loss formula does not account for Oxygen absorption or rain induced absorption. When factoring Oxygen absorption of 16dB/Km and rain induced fading whose strength depends on the desired availability, we get the results shown in the graph below.

© RAPID5G Consortium

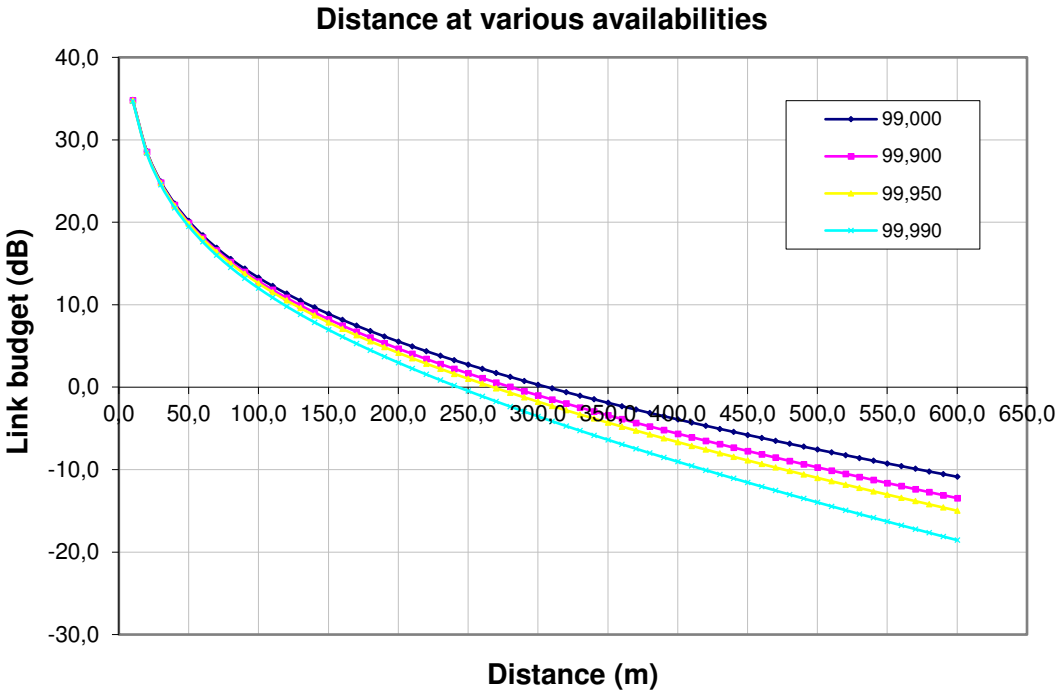

Figure 5: Calaulated link distance at various availability

As can be seen from the graph above, the achievable link distance with 25dBi antenna assuming clear line-of-sight is between 250m and 300m, which represents a reasonable cellular cell size.

© RAPID5G Consortium

5 Beam-steering architectures

Beam steering is the capability to direct the electromagnetic wave radiated from an antenna to a desired direction. There are various performance related parameters associated with beam-forming, which are summarised in the table below.

Parameter	Description
Steering range	The angular range (azimuth and elevation) across which the beam can be steered
Gain angular variation	The variation in the gain of the antenna across is steering range
Steering resolution	The resolution by which the beam can be steered to a desired direction within the steering range
Beam directivity	The directivity of the beam when steered to a specific direction
Spurious side lobe level	The level of spurious side lobes generated by the steering operation
Coherence bandwidth	The size of the widest chunk of spectrum which could be steered simultaneously to the same direction
RF power efficiency	The portion of the power the is injected to the antenna that is eventually radiated
Steering speed	The time duration it takes to change the beam direction
Physical dimension	Physical size of the antenna (typically as compared to the wavelength)
Architectural impacts	Impacts of the antenna on the overall system design
Ease of construction	The complexity of commercially manufacturing the antenna

Table 3: Beam-steering antenna performance parameters

Over the years, a large variety of techniques have been proposed to perform beam-steering. The following sections describe these techniques.

5.1 Beam-forming

Beam-forming is probably the best known beam-steering method. The method is based on the usage of an array of radiating elements which are fed by the signal to radiate, but each element receives the signal at a specific power and phase, such that the combined radiation from the array a coherent wave front at the desired direction of propagation. The control of individual radiating element amplitude and phase can be done either at base-band, IF or RF, and results in different complexity of implementation and different performances ([4], [10]). The table below describes the antenna performance parameters for beam-forming at mm-wave frequencies.

Parameter	Description
Steering range	Assuming an array composed of identical elements, the steering range is defined by the radiation power envelope of the radiating element. Typical radiation elements (patches, dipoles, slots) can easily reach steering range in excess of 90°. Steering range in excess of 180° would typically require arranging the elements on a non planar surface
Gain angular variation	Typically follows the radiation power envelope of the radiating element
Steering resolution	Derived from the resolution of controlling the radiating elements phase
Beam directivity	Assuming equal power at the radiating elements, it is roughly proportional to $10 \cdot \log_{10}(N)$ where N is the number of radiating elements
Spurious side lobe level	Strongly depends on the number of radiating elements as well as the distance between them and the power tapering applied to the elements
Coherence bandwidth	Depends on the way the phase differences are implemented. When implemented by true time delay the bandwidth is limited by the bandwidth of the radiating elements
RF power efficiency	Potentially very high, depending on the exact implementation. Power may be lost in the feeding network, especially if split multiple times. In case of using multiple power amplifiers to reduce the amount of power splitting loss may be low
Steering speed	As fast as the power and phase to the radiating elements can be varied. Typically in mm-wave implementations that would be within nanoseconds
Physical dimension	May be very compact. Typical radiating element distance is $\lambda/2$ which is 2.5mm at 60GHz, so an array of 4x8 elements yielding about 25dBi gain would roughly be 20mm x 10mm in size
Architectural impacts	In mm-wave implementations radiating elements are typically fed by a dedicated PA. This enables radiating significantly more power than a single PA serving all elements

© RAPID5G Consortium

Parameter	Description
Ease of construction	Radiation directly from a mm-wave chip is hard to implement due to the size of the chip as compared to the size of the array. Typically the radiating elements are implemented as part of the package, facilitating tight integration between the chip and the radiating elements. Loss and phase errors in the feeding network should be carefully observed

Table 4: Beam forming performance parameters

5.2 Lens/reflector assisted beam-switching

The beam-switching method ([5]) is based on the usage of an array of radiating elements positioned on the focal plane of a radiation focusing element. Such an element could be a dielectric lens, in which case the radiators array is positioned behind the lens and radiates through the lens, or a reflector, in which case the radiators array is positioned in front of the reflector and might created blockage to the radiation reflected from the reflector. In this method the position of the radiating element (or elements) determines the direction the coherent wave front emanating from the antenna. The radiated pattern is determined primarily by the passive focusing element. The radiating elements should illuminate the passive element with a reasonable power taper and minimal spillover in order to get an output beam with low side lobes. The control of the radiating elements includes only turning them on or off, so power control and phase control circuits are eliminated, thus simplifying the radiating array design. The table below describes the antenna performance parameters for switching-forming at mm-wave frequencies.

Parameter	Description
Steering range	The steering range is defined by the amount of radiating elements and the beamwidth of the antenna, i.e. if the antenna horizontal beamwidth is 2° and there are 10 elements in the horizontal direction, they will facilitate a horizontal steering range of 20° degrees
Gain angular variation	The gain degrades when moving from the passive element axis due to less efficient illuminating by the radiating elements that are farther from the axis
Steering resolution	Determined by the distance between the radiating elements relative to the focal length of the passive element
Beam directivity	Determined by the area of the passive element
Spurious side lobe level	Very good side lobe level can be achieved when decent illumination taper is used and spillover is avoided by the radiating elements
Coherence bandwidth	Unlimited
RF power efficiency	Potentially very high. Some power may be lost in the dielectric lens in case such a lens is used
Steering speed	As fast as the radiating elements can be switched. Typically in mm-wave implementations that would be within nanoseconds
Physical dimension	Depends on the desired gain and similar to a passive antenna. A 25dBi gain beam switching lens antenna would have a diameter of about 38mm. The focal distance of the passive focusing element determines the thickness of the antenna
Architectural impacts	Driving the radiating elements by a dedicated PA enables eliminating switching losses. Specific arrangements of the elements on the focal plane enable fine control on the scan pattern and scan resolution. Typically no calibrations are required
Ease of construction	Radiation directly from a mm-wave chip is hard to implement due to the size of the chip as compared to the size of the array. Typically the radiating elements are implemented as part of the package, facilitating tight integration between the chip and the radiating elements

Table 5: Beam switching performance parameters

5.3 Travelling wave

Travelling antenna are antennas in which the electromagnetic wave propagates without reflections due to the antenna being terminated. This creates a well defined distribution of electric and magnetic field within the antenna which in turn enables coupling the electromagnetic energy to an array of radiating elements. A typical construction would consist of a waveguide where the radiating elements are slots in the waveguide ([6]). The phase difference between the radiating elements depends on their distance (and is hence frequency dependent) while the power taper depends on the portion of power coupled into

© RAPID5G Consortium

the elements. Travelling wave antenna may also control the phase of the radiated wave by using controllable loading of the radiating elements, thus achieving control on the scanning direction which is not frequency dependent ([7]).
The table below describes the antenna performance parameters for travelling wave antennas at mm-wave frequencies.

Parameter	Description
Steering range	The steering range is defined by the number and arrangement of radiating elements and is typically directly related to the frequency of the radiated wave
Gain angular variation	The angular variation might be degraded by differences in power coupling resulting from the fact the steering angle is typically frequency dependent
Steering resolution	Excellent steering resolution may be achieved by varying the radiated frequency
Beam directivity	Determined by the number of radiating elements
Spurious side lobe level	Very good side lobe level can be achieved due to good control on the number of radiating elements and the power taper applied to them
Coherence bandwidth	Narrow, different frequencies typically radiate in different directions
RF power efficiency	Potentially very high. Some power is lost to the termination assuring the travelling wave nature of the antenna
Steering speed	As fast as the frequency can be scanned
Physical dimension	May be very compact. Typical radiating element distance is $\lambda/2$ which is 2.5mm at 60GHz, so an array of 4x8 elements yielding about 25dBi gain would roughly be 20mm x 10mm in size
Architectural impacts	The most significant impact is the frequency dependence of scanning angle which limits the application suitable for this type of scanning
Ease of construction	Typically the radiating elements are implemented as part of the feeding waveguide. Ease of construction depends on the type of wave guide being used. Low loss waveguides are easy to utilize and facilitate high efficiency

Table 6: Travelling wave performance parameters

5.4 Tunable reflect-array

A reflect array antenna is similar to a reflector based antenna in the sense that a radiating source is pointed towards the reflector which is utilized to focus the beam and direct it to the desired direction. Unlike a reflector, the reflect array is composed of multiple reflecting element such that each element may reflect the wave front incident upon it with a unique phase shift. The phase shifts are selected such that a coherent wave front is generated at the desired direction of propagation. In order to use the reflect array for mm-wave beam-steering, the phase shift of the reflecting elements needs to be tunable, for instance, by using phase shifters ([11]), which may be statically or dynamically defined.
The table below describes the antenna performance parameters for beam-forming at mm-wave frequencies.

Parameter	Description
Steering range	The steering range is defined by the radiation power envelope of the radiating elements, which is typically in excess of 90°
Gain angular variation	Typically follows the radiation power envelope of the radiating element
Steering resolution	Derived from the resolution of controlling the radiating elements phase
Beam directivity	Typically related to the area of the reflection surface, the effective area constituting an order of 30-50% of the physical area. The area and thus the directivity are limited by phase errors caused by the fact that the reflecting area is typically flat rather than parabolic
Spurious side lobe level	Low spurious and side lobe level can be achieved by proper tapering if the radiating source exciting the reflector
Coherence bandwidth	Depends on the way the phase differences are implemented, but typically limited by phase errors caused by the fact that the reflecting area is flat rather than parabolic
RF power efficiency	Typically high. Some power loss is may be caused by the phase shifters
Steering speed	As fast as the phase shifters can be varied. Typically in mm-wave implementations that would be within nanoseconds
Physical dimension	Depends on the desired gain, which is directly related to the physical area. For 40% efficiency and 25dBi gain at 60GHz an area of 20mm x 20mm would be required
Architectural impact	The source illuminating the reflect array must be placed in front of it, thus complicating construction. The source may generate an obstruction that requires either on offset construction of enlarging the reflect array size

© RAPID5G Consortium

Parameter	Description
Ease of construction	The reflect array itself is easy to construct. Controllable phase shifters are much more complex, and typically hard to integrate into an RFIC without incurring significant losses

Table 7: Tunable reflect array performance parameters

5.5 Meta-material

Meta-material are engineered surfaces designed to exhibit an effective permittivity and permeability which can be tuned to positive and even negative values. Such tuning affects the refractive index and can be done by using active elements such as diodes and transistors or using MEMS technology ([8], [9]). The capability of tuning the refractive index enables generating reflective or transmissive surfaces which can deflect a plane wave incident upon them, thus resulting in beam steering action, without the use of complex designs for feeding and phase shifting networks. Although this technology is promising, it is quite new, and not widely used, especially not in the mmwave spectrum frequency range.

5.6 Liquid Crystal

Liquid crystal panels can be manufactured at very low cost due to their extensive use as display device in various industries. The liquid crystal panel has the capability the change the polarization of elements on the panel and thus modulate their reflectivity and consequently their phase. The capability of fine spatial control on the reflection by the panel enables generating reflective surfaces which can deflect a plane wave to a desired direction just by controlling the polarization of the liquid crystal elements on the panel ([12]). This technology is very promising in terms of manufacturability and cost as well as achievable performance. However, it is far from maturity and still requires considerable research in order to apply it in the mmwave spectrum frequency range.

© RAPID5G Consortium

6 Antenna design

6.1 Travelling wave antenna (UDE)

6.1.1 Operation principle of the passive PCB antenna

The proposed passive PCB antenna uses the travelling wave concept. It is based on a leaky-wave substrate-integrated waveguide, consisting of a periodic array of N unit cells. The unit cell is a SIW designed for a lower cutoff frequency of 40 GHz, from which two rectangular slots are removed off the top metal plane to create a planar dipole. The printed dipoles are placed longitudinal to the direction of wave propagation, which feeds the radiating dipoles, as depicted in Figure 6. The length of the printed dipoles corresponds to a guided wavelength of 61.3 GHz in the middle of the 57-66 GHz band, where the antenna is designed to exhibit broadside radiation.

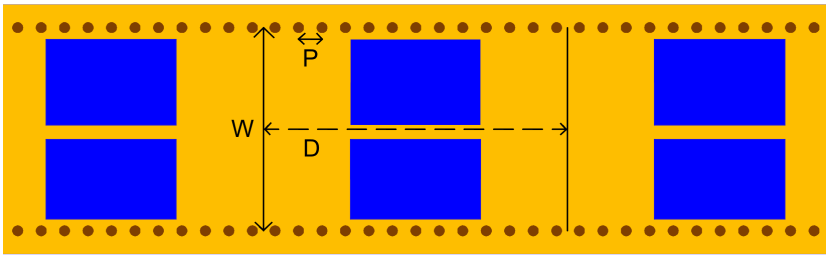

Figure 6: Drawing of the passive PCB LWA based on Rogers RT/duroid® 5880; the unit cell period D is 3.9 mm, the via holes (brown) have a diameter of 0.15 mm and a pitch P of 0.3 mm, the SIW has a width W of 2.6 mm.

Similar to a phased array antenna the beam angle depends on the wavelength of the radio signal and the distance, which corresponds to the periodicity, and the phase difference between radiating elements. In this design the dispersion of the LWA is employed to create a frequency dependant phase difference and thereby create beam steering. As depicted in Figure 7 the SIW inherits an almost linear dispersion characteristic. Another advantage of the SIW is its low loss, which allows for a good power taper between the radiating elements.

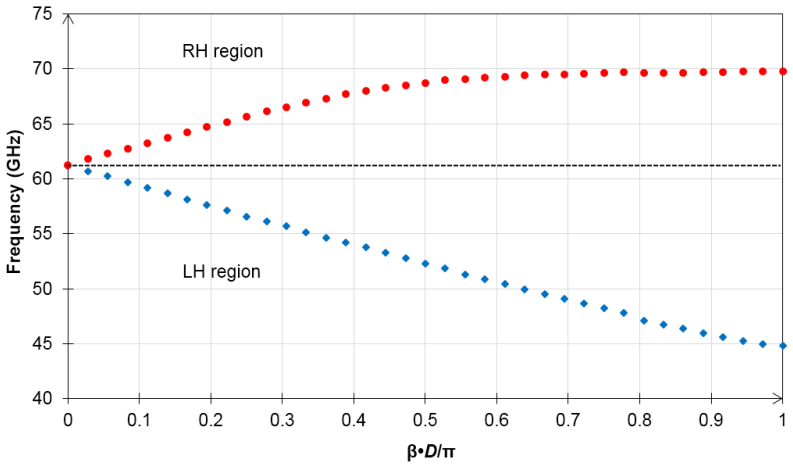

Figure 7: Dispersion diagram from Eigenmode simulations, showing the modes and their frequencies corresponding to the RH and LH regions over the normalized phase coefficient times the unit cell periodicity D

© RAPID5G Consortium

In order to access the SIW and remove the DC short between ground and signal for the interface, a coupled line transition from SIW to GCPW has been designed. The transition also provides impedance matching from the SIW to the 50 Ohm GCPW interface.

6.1.2 Physical construction of the passive PCB antenna

The antenna has been fabricated using Rogers RT/duroid® 5880 laminate and standard PCB processes. Antennas with 12 and 20 dipoles have been fabricated as well as an antenna with 4 arrays with 12 dipoles each, which also contains power dividers. In order to provide a coaxial RF interface commercial end-launch connectors are used. Brass holding brackets are also manufactured to fix the antenna.

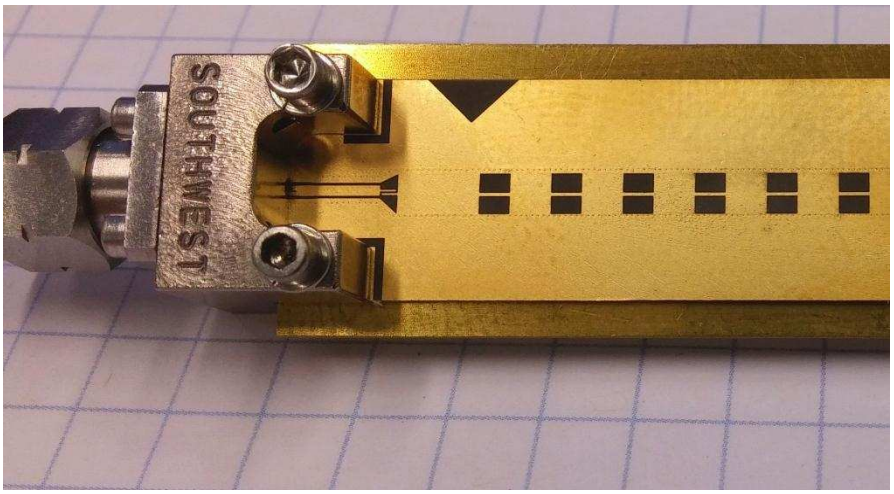

Figure 8: Fabricated LWA with printed dipoles, coupled-line transition and end-launch connector providing a coaxial interface

6.2 Beam switching antenna (Siklu)

6.2.1 Operation principle

The method selected for the beam steerable antenna is the lens assisted beam switching method. Two prototypes where constructed, each based on an array of radiating elements implemented on a proper laminate. In each prototype the substrate hosting the radiating elements has been positioned on the focal plane of a mm-wave lens.
The beam switching method has some advantages over other implementation methods, specifically when considering a moderate number of radiating elements. The major advantage is the fact that the radiated pattern is determined primarily by the mm-wave lens, which is a passive device. Thus the radiation pattern as well as the gain of the antenna is determined by the size of the lens and the design of the illumination taper across it. The beam-steering action is achieved by simple turn-on or turn-off of specific radiating elements, thus no power control and phase control circuits are required, greatly simplifying the driving RFIC and the feeding networks. The fact that only a single RF chain needs to be active is an additional benefit, enabling reduction in power consumption and size of the mm-wave driving RFIC.
The diagram below provides a schematic illustration to the lens assisted beam steering concept.

© RAPID5G Consortium

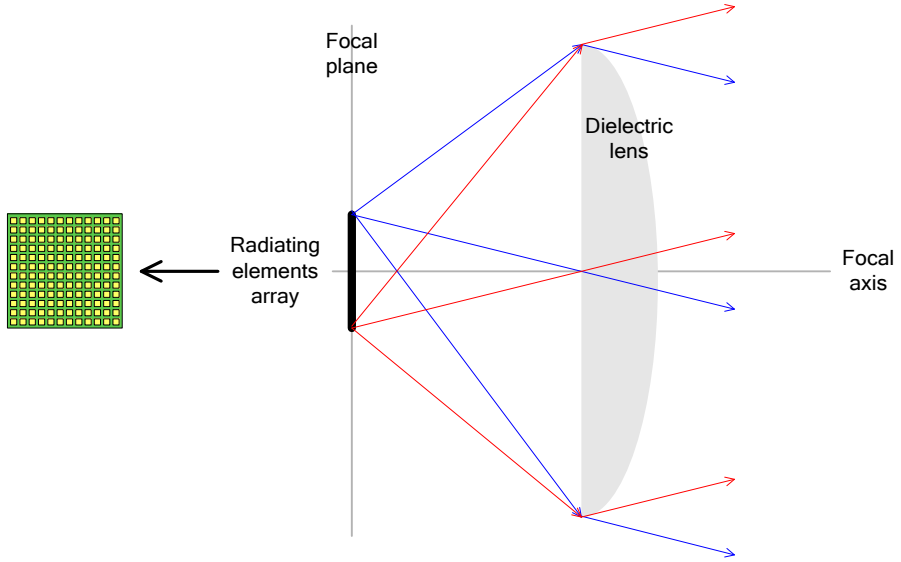

Figure 9: lens assisted beam-switching schematic view

While the beam characteristic in the above concept is primarily determined by the lens, the beam steering performance is determined by the number of elements and their arrangement on the focal plane. The radiating element polarization is preserved while going through the lens, so in principle this concept can easily accommodate use of the alternate polarization as a parallel operating beam steering antenna using the same focusing lens. The diagram below illustrates the geometry considerations associated with the beam steering range.

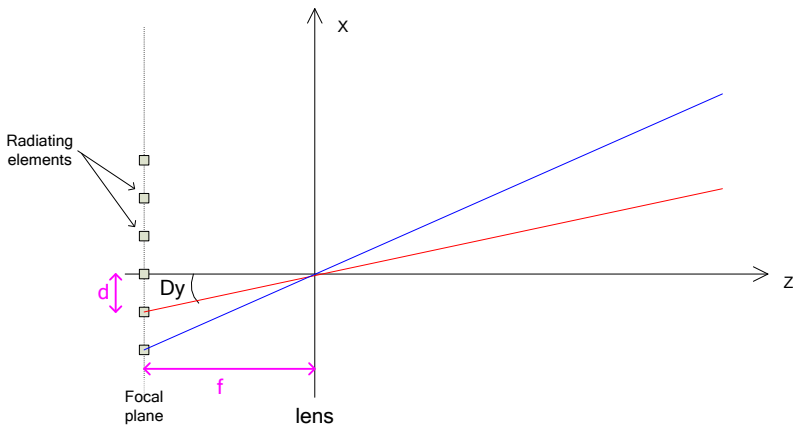

Figure 10: lens assisted beam-switching geometry

The beam steering action is determined by the focal distance of the lens and the distance between the radiating elements. The beam angular difference between two adjacent elements is determined by $\Delta\psi = \arctan\left(\frac{d}{f}\right)$ where d is the distance between two adjacent radiating elements and f is the focal distance of the lens. It follows the if we place a M x N array on the focal plane we get a scanning range of $M\cdot\Delta\psi$ in one direction and $N\cdot\Delta\psi$ in the perpendicular direction. The element arrangement on the focal plane

© RAPID5G Consortium

could also take other shapes than a rectangular grid, in accordance with the desired scanning characteristics.

6.2.2 Physical construction

Two antenna constructions based on the beam-switching concept were examined in order to test and demonstrate the beam steering operation. The first construction has the radiating elements on a PCB material based substrate, such that the radiating elements can be fed directly through a waveguide interface. The second construction has the radiating elements on LTCC material based substrate, such that the radiating elements are fed from an RFIC mounted on the same substrate.

6.2.2.1 PCB based construction

The PCB based construction enables evaluating the performance of radiating elements implemented on soft, organic laminates, which are laminated together using standard PCB manufacturing process. The PCB process is commercially cheap, and has certain limitations with regards to feature size and accuracy. The radiating elements are directly connected to a waveguide interface, thus an exact power level can be injected into the radiating elements and the exact power level it receives can be measured. The PCB construction is limited by the fact the waveguide interface is physically large related to the overall radiating array size, so the number of active elements in the array is limited by the number of waveguide interfaces instances that can be placed around it.
The figure below shows the PCB construction from the radiating element direction and from the feeding structure direction.

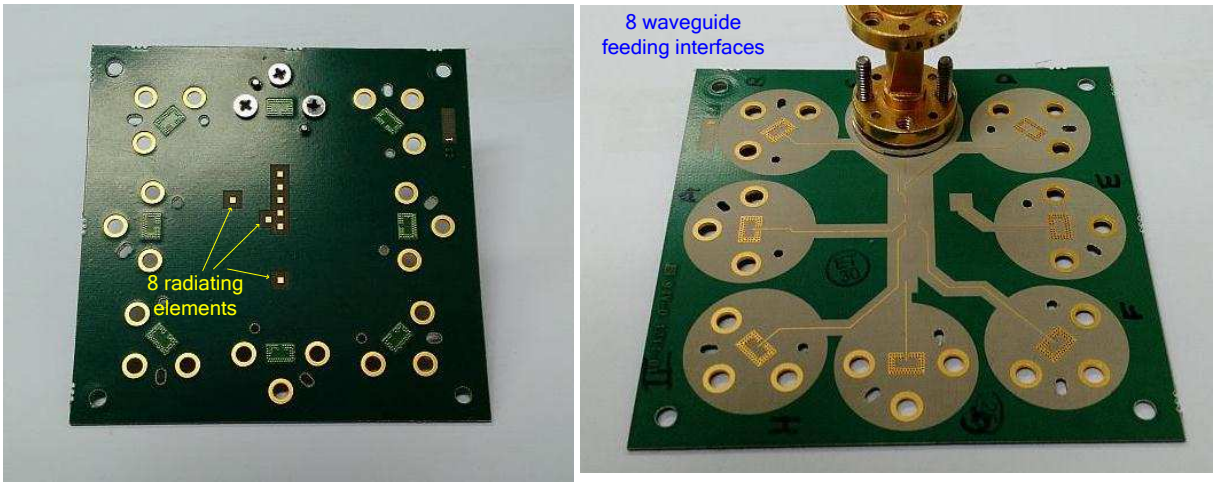

Figure 11: PCB with radiating elements (top and bottom)

The 8 elements shown in the picture above are part of a full design containing 61 elements arranged on a hexagonal grid. The picture of the full grid is shown below, with the elements that are actually present marked in black. The elements actually implemented were selected such that the vertical and horizontal scanning step can be demonstrated as well as the full vertical and horizontal scanning range.

© RAPID5G Consortium

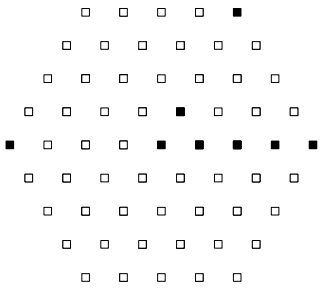

Figure 12: PCB full grid design

The figure below shows the entire construction which includes the PCB with the radiating elements as well as the passive lens.

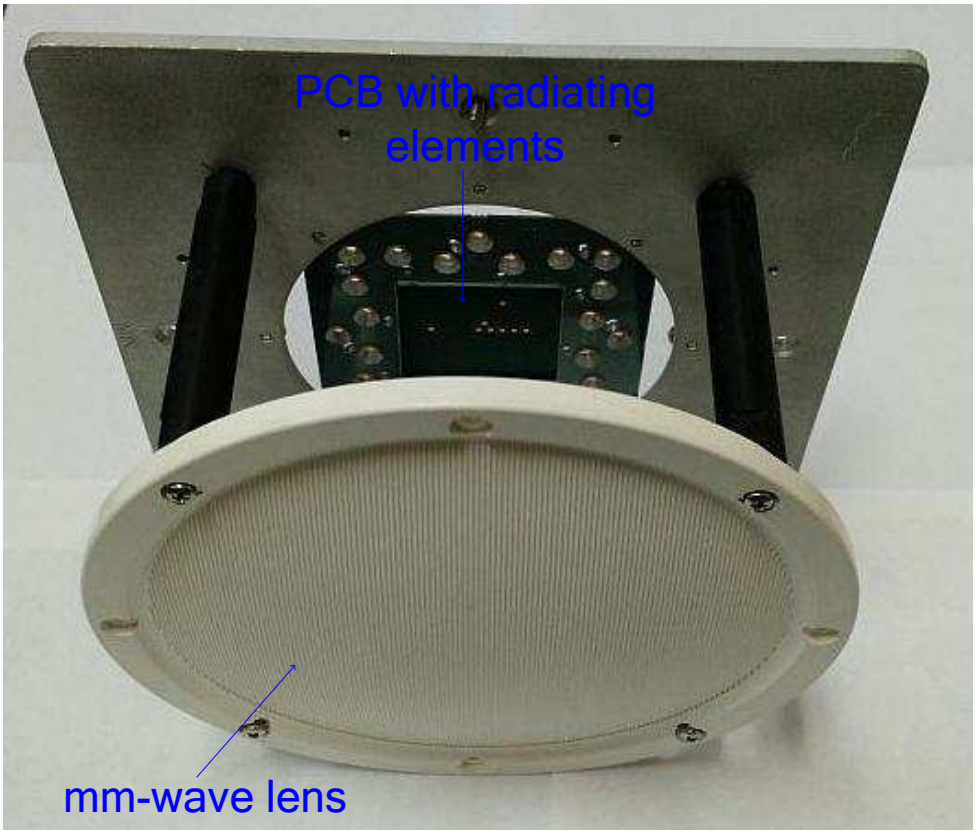

Figure 13: PCB based full antenna construction

6.2.2.2 LTCC based construction

The LTCC based construction enables demonstrating the actual performance of a fully populated array. The radiating elements are implemented on ceramic LTCC material which is laminated using a low-temperature co-firing manufacturing process. The LTCC process is commercially more expensive than the PCB process, but it is capable of feature size and accuracy that are required in order to install the RFIC on the laminate.
In this construction the radiating elements are directly connected to the RFIC, and therefore their direct evaluation is not possible. As an alternative, another RFIC is installed on the same laminate with an interface that enables measuring its output power by using dedicated mm-wave probes. Using this method, the problem that we cannot excite the

© RAPID5G Consortium

radiating elements with an exact power level is somewhat overcome, as we can measure the power level from the secondary RFIC and assume it is close to the power level from the primary RFIC. The array features 32 radiating elements which can all be excited, thus demonstrating actual beam-steering operation covering the full beam-width supported by the design.
The figure below shows the LTCC construction from the radiating element direction and from the feeding RFIC direction.

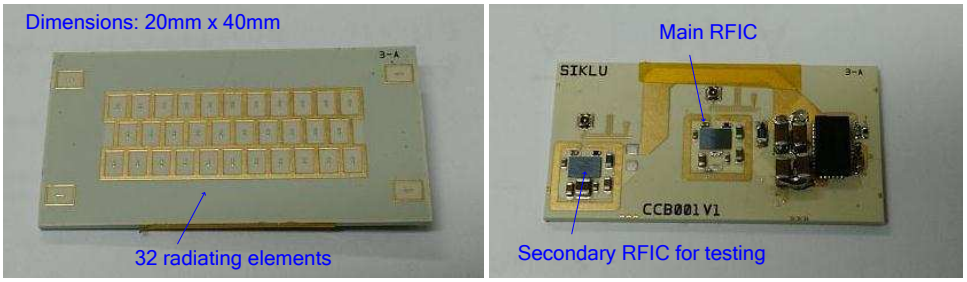

Figure 14: LTCC with radiating elements (top and bottom)

The 32 elements on the array are arranged in three rows with 11, 10 and 11 elements, to enable beam steering in both horizontal and vertical directions. The figure below shows the entire construction which includes the LTCC with the radiating elements as well as the passive lens in a mechanical enclosure.

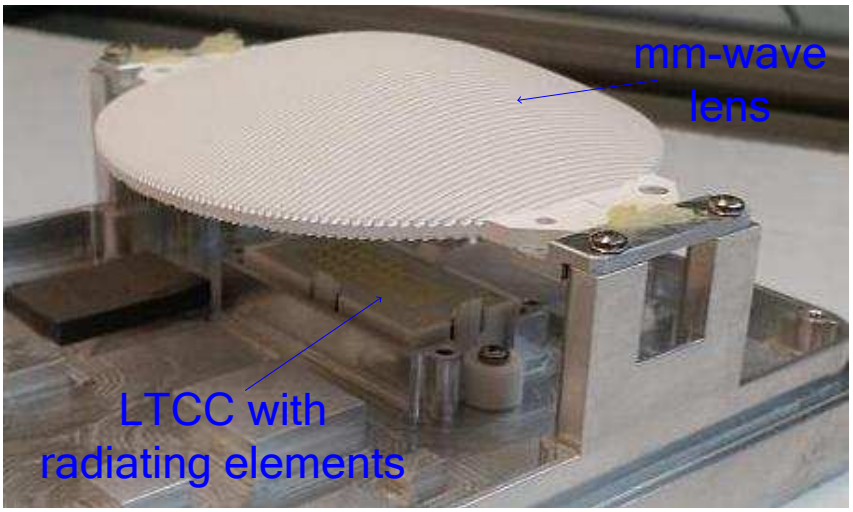

Figure 15: LTCC based full antenna construction

© RAPID5G Consortium

6.3 Electro-optical beam-steering antenna (Osaka)

6.3.1 Principle of operation

The electro-optical antenna will be reported in detail in D322. However, the principle of operation is already explained here to give a comprehensive overview of the chosen technology.

A space-division-multiplexing (SDM) technique is useful for preparing a lot of wireless channels to support dense user environments. Especially, in millimeter-wave (MMW) band wireless system, the wireless channels can be multiplexed densely due to small diffraction property of MMW. OSAKA have proposed and developed array-antenna-electrode (AAE) electro-optic (EO) modulators for converting SDM wireless signals to optical signals with interesting beam forming characteristics. The AAE-EO modulators can receive MMW wireless signals and convert them to optical signals without external power supply. In addition, the directivity in the wireless-optical signal conversion can be controlled by introducing polarization-reversed patterns. By fabricating multiple optical waveguides with different polarization-reversed patterns in the substrate of an AAE-EO modulator, multiple SDM signals can be received and discriminated simultaneously by using a single AAE-EO modulator.
A new technique to double SDM channel numbers discriminated by using the AAE-EO modulator is shown below.

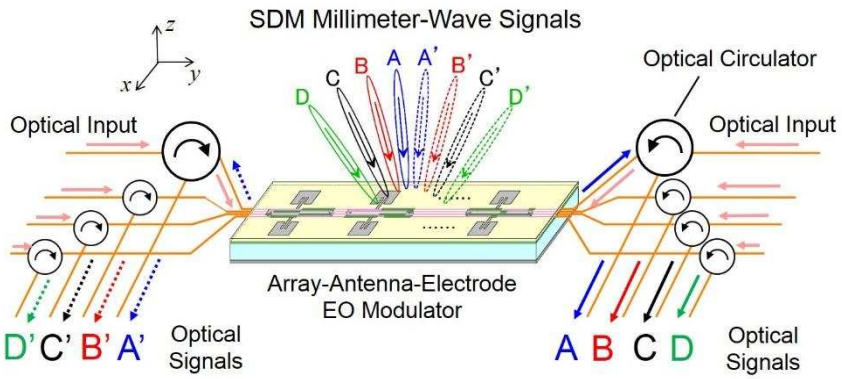

Figure 16: Discrimination of SDM channels by using AAE-EO modulator

Several polarization-reversed patterns can be introduced to an optical waveguide in order to enhance the conversion efficiency for the wireless signal coming from at an angle of θ. In this research project, OSAKA found a useful technique for selecting polarization-reversed patterns, where an even-symmetric polarization-reversed pattern from its center is to be used for doubling SDM channels. Then, the modulation efficiency for the light-wave propagating along $+y$ direction in the optical waveguide introduced the even-symmetric polarization-reversed pattern can be selectively enhanced when the wireless signal is coming from the direction of $+\theta$ while its modulation efficiency is rather small for wireless signals coming from other directions. On the other hand, the modulation efficiency for the light-wave propagating along $-y$ direction in the same optical waveguide can be selectively enhanced when the wireless signal is coming from the direction of $-\theta$. Therefore, two MMW wireless signals with incident angles of $\pm\theta$ can be received by use of only single optical waveguide with the even-symmetric polarization-reversed patterns with optical circulators as shown in Figure 16. In the same figure, up-to 8 SDM channels can be discriminated using a single AAE-EO modulator with four optical waveguides with corresponding even-symmetric polarization-reversed patterns.

© RAPID5G Consortium

An illustration of the designed directivity is shown below. The peak angles and beam widths can be almost arbitrarily designed by adjusting the polarization-reversed patterns, number of antenna-electrode elements, and the interval between adjacent antenna-electrodes.

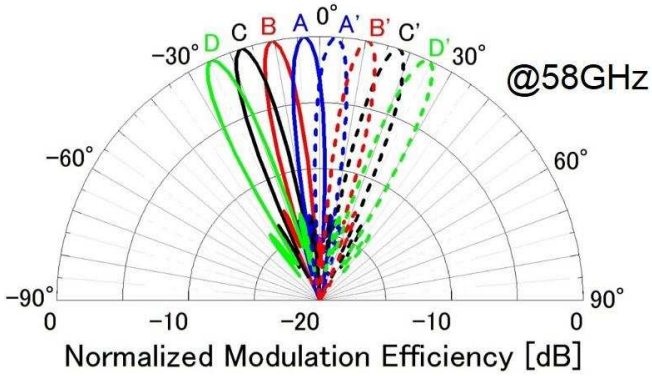

Figure 17: The designed directivity on MMW wireless/optical signal conversion

© RAPID5G Consortium

7 Design verification setup

The design verification for the beam steering antenna consists primarily of measuring the achieved antenna performance. The antenna performance can be characterised in terms of radiation efficiency (i.e. what portion of the RF power injected to the antenna is eventually radiated) and in terms of antenna pattern, where this pattern is measured for specific beam steering directions spanning the beam steering coverage range of the antenna.
The antenna radiation efficiency is measured by comparing to a reference antenna with known gain. The antenna pattern is measured by placing the antenna on a mechanical rotator than can rotate both in the azimuth and elevation axis. A receiving antenna connected to a spectrum analyzer is placed opposite to the antenna under test, at a distance which is higher than the far field limit of both antennas. The far field limit is given by $2 \cdot D^2/\lambda$ where D is the largest antenna dimension and λ is the wavelength equal to about 5mm at the 57-64GHz band. For the antennas under test, the largest antenna dimension is about 90mm, placing the far field threshold at about 3m. The antenna under test is excited at the desired measurement frequency and the rotator is rotated across the desired angular sweep while taking measurements of the received power at the measurement antenna. The setup diagram and picture are shown below.

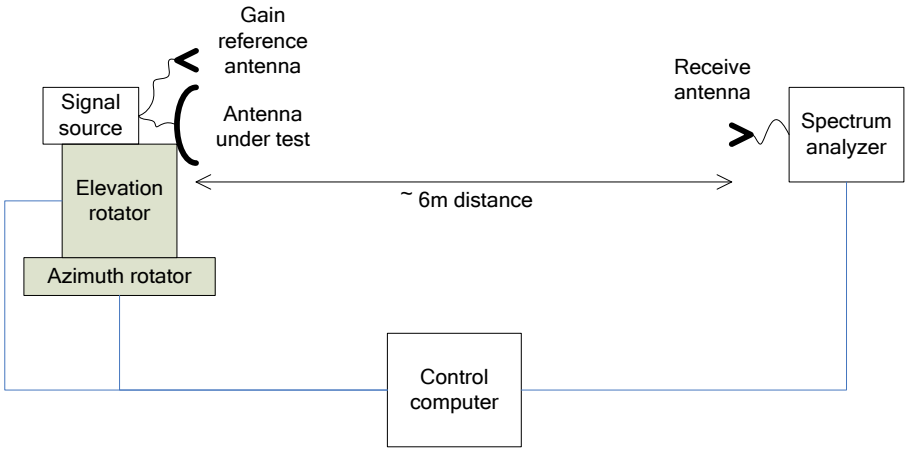

Figure 18: Schematic measurement setup

© RAPID5G Consortium

8 Design verification results

8.1 Travelling wave antenna (UDE)

8.1.1 Verification of the passive PCB antenna

The design verification process consists of measuring the radiation pattern of the fabricated antenna and calculating its gain by comparing its performance to a calibrated horn antenna with known gain. Initial measurements were conducted by UDE using a photodiode as an RF source that demonstrate the beam steering capabilities of the antenna as shown in *Figure 19*.

After confirming the functionality of the antenna further measurements have been conducted by ENRI in their anechoic chamber to yield precise results. These measurements using a vector network analyser (VNA) and a V-band extender module are presented in the following.

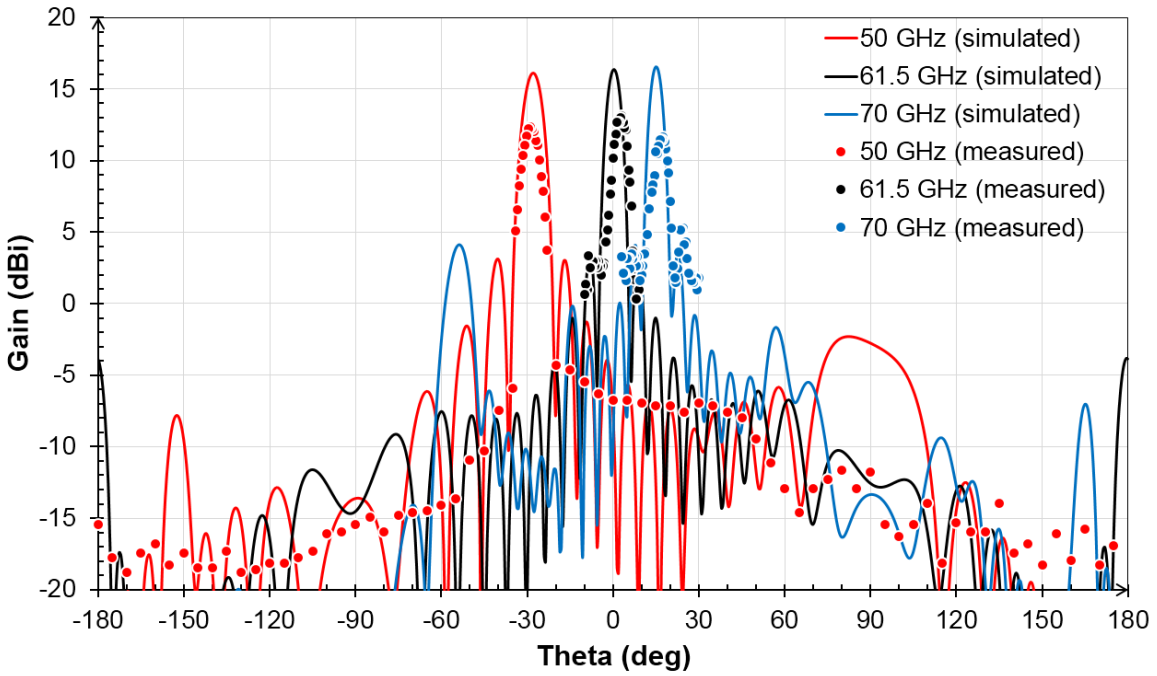

Figure 19: Radiation patterns showing the simulated (solid lines) and measured (circles) gain of the travelling wave antenna at 50 GHz (red), 61.5 GHz (black) and 70 GHz (blue).

8.1.2 Verification results for the passive PCB antenna

For the measurements the LWA is excited at its coaxial feeding port with a single frequency signal. The frequency is then changed in 1 GHz steps from 50 GHz to 67 GHz.
The graph below (*Figure 20*) shows the maximum obtained gain for frequencies between 50 GHz and 67 GHz for the LWAs with one and four arrays of 12 dipoles each. As can be seen the gain is relatively flat in this frequency range with around 12 dBi for the one array LWA and around 16 dBi for the four array LWA, including power splitters. No major degradation of gain can be observed around broadside frequency at 61 GHz. Therefore it is concluded, that the designed asymmetry to reduce the open stopband behaviour of the LWA has been effective.

© RAPID5G Consortium

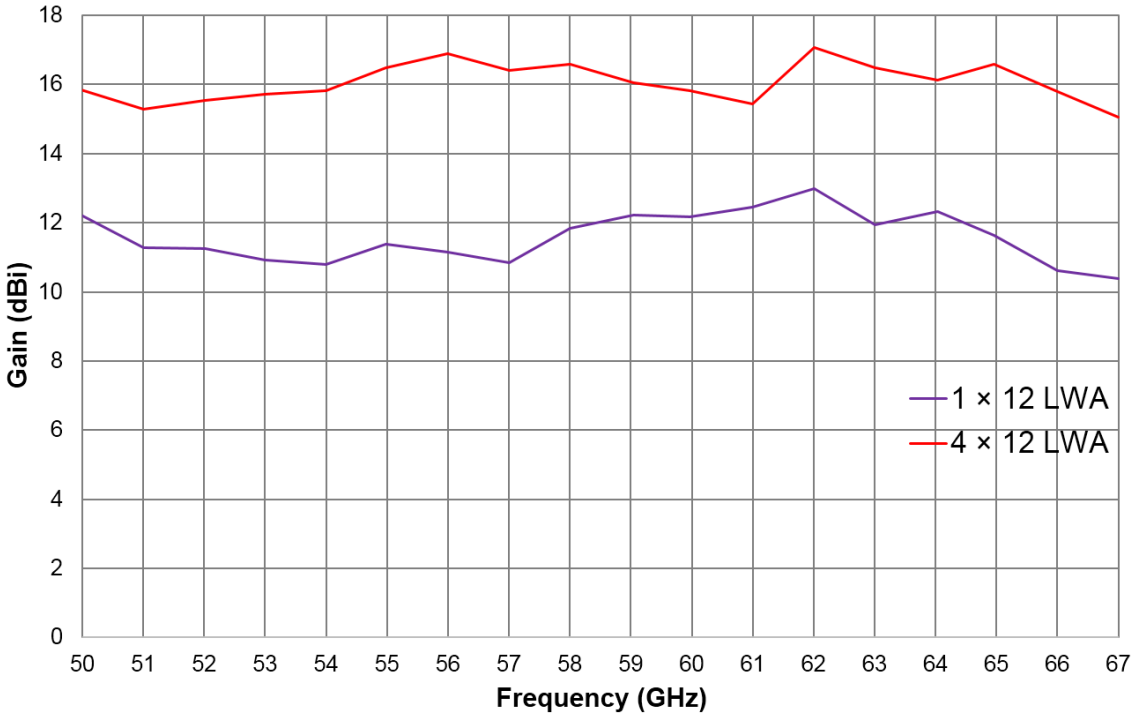

Figure 20: Frequency response of the travelling wave antenna with one and with four arrays of 12 dipoles each, plotted as the gain over the frequency from 50 to 67 GHz.

In *Figure 21* the E-plane radiation pattern of the LWAs at 61 GHz near the broadside frequency is depicted. For the LWA with one array the observed pattern is comparable to that of a single printed dipole with little directivity in the E-plane. For the four array LWA a mainlobe and distinct sidelobes can be observed, until the pattern equals that of the one array LWA for angles greater than +/- 90 degree.

© RAPID5G Consortium

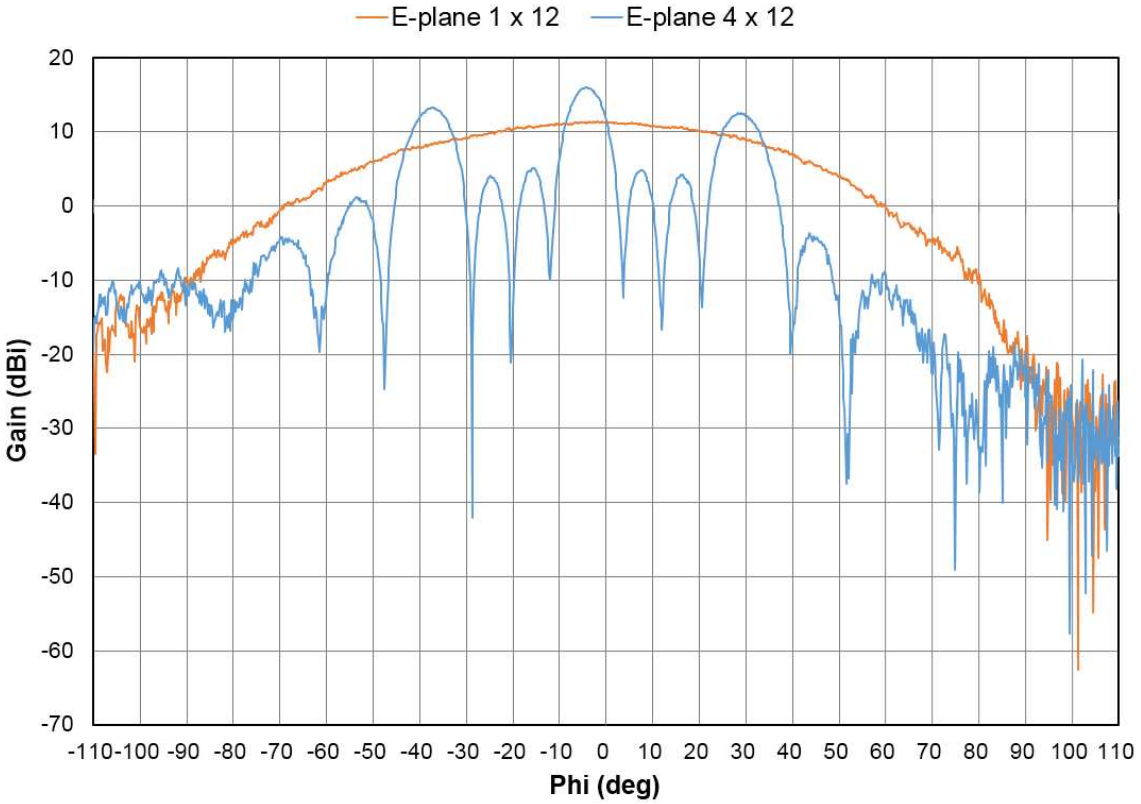

Figure 21: Radiation pattern of the E-plane LWAs with one and four arrays of 12 dipoles each as gain in dBi over beam angle between -110 and +110 degrees at 61 GHz.

In *Figure 22* the H-plane radiation pattern of the 12 elements LWA with a single array is depicted. It shows the simulated as well as the measured gain between -50 and +50 degrees beam angle at the frequencies 50 GHz, 57 GHz, 61 GHz and 66 GHz. From the beam angle change of the gain peak with changing frequency, the beam steering behaviour of the LWA can be observed. The maximum gain for 57 GHz is at -9.8 deg, for 61 GHz at -0.6 deg and for 66 GHz for 8.4 deg, respectively. Thereby 18.2 degrees of beam steering are obtained in the frequency range of interest from 57 GHz to 66 GHz. Overall over 40 degrees of beam steering over frequency are measured using the LWA. Furthermore figure 10 demonstrates good agreement between the simulated and measured values. Only a slight shift of the beam angle and around 4 dB difference in gain are observed.
For the single array antenna, the 3 dB beam widths in the E-plane and H-plane are 60° and 6°, respectively. For four array antenna they are slightly smaller.

© RAPID5G Consortium

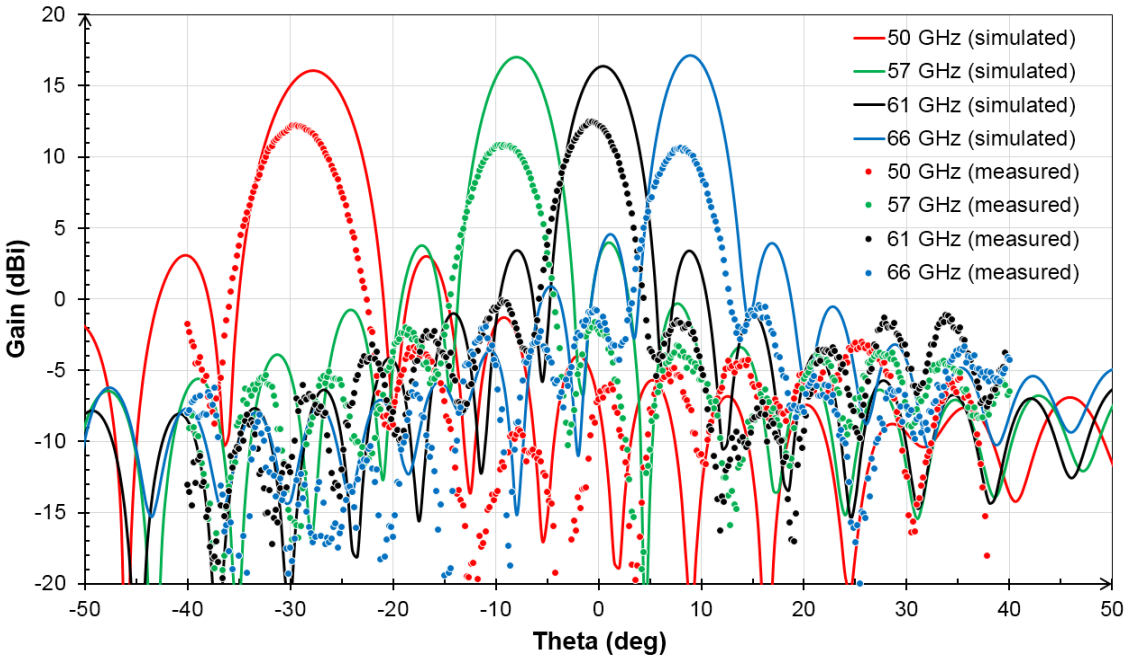

Figure 22: Gain over frequency and scanning operation for travelling wave antenna

8.2 Beam switching antenna (Siklu)

8.2.1 PCB based construction

8.2.1.1 Individual beam patterns

The graph below shows the measured beam patterns resulting from exciting the elements along the horizontal axis. Each element is excited separately and each generates a distinct beam direction. The antenna patterns differ in gain level mainly due to different length of trace wire connecting the radiating element to the feeding point (typical attenuation on the PCB is ~1.5dB/cm).

© RAPID5G Consortium

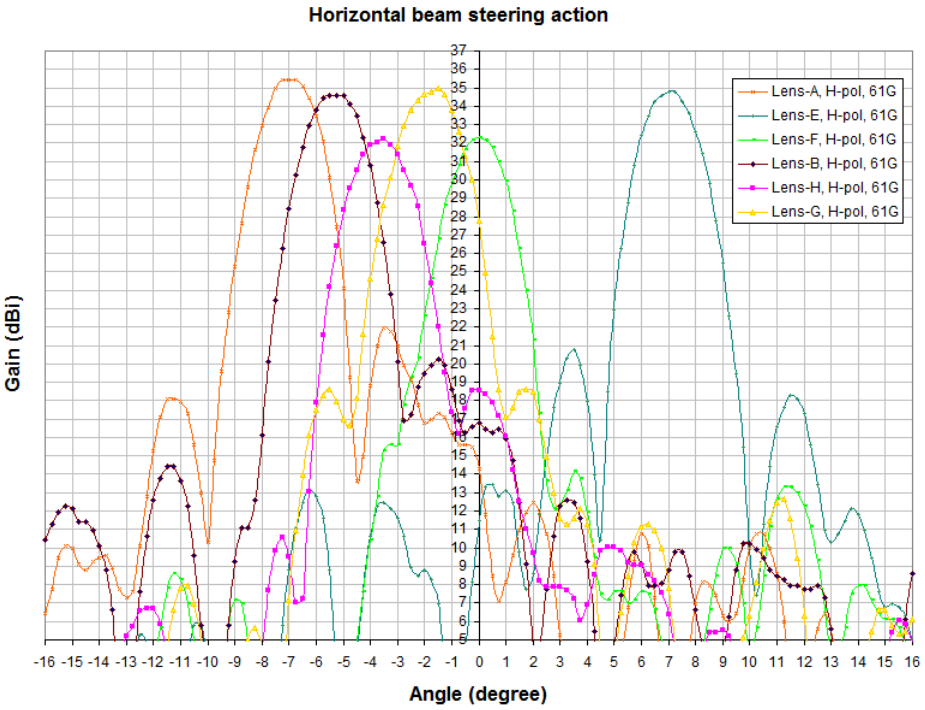

Figure 23: Horizontal scanning beams

The graph below shows the measured beam patterns resulting from exciting the elements along the vertical axis. Each element is excited separately and each generates a distinct beam direction. Since the mechanical scanner must first perform the vertical sweep and then the horizontal sweep, the entire antenna is rotated by 90° in order to perform this sweep. Here again, the antenna patterns differ in gain level mainly due to different length of trace wire connecting the radiating element to the feeding point.

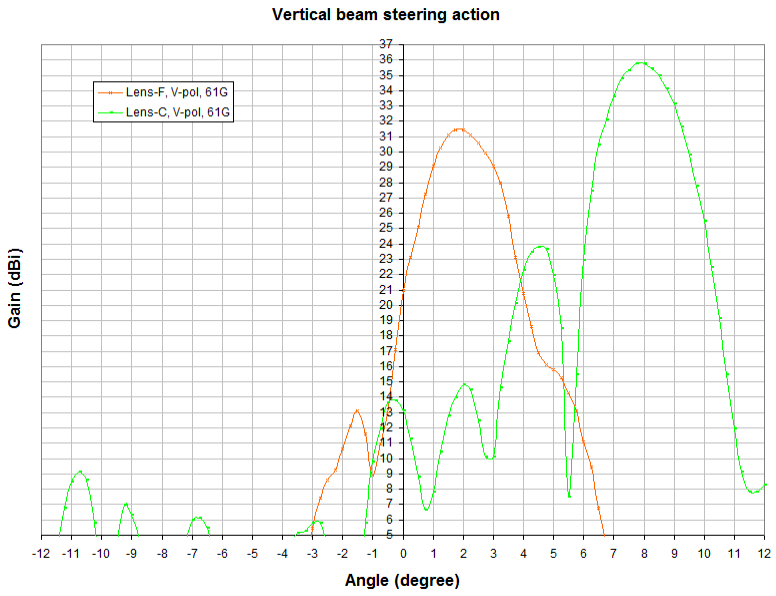

Figure 24: Vertical scanning beams

© RAPID5G Consortium

From the two graphs above it may be concluded that the horizontal scanning range of the antenna would be ±8° (to the -3dB point) while the vertical scanning range would be ±9°. The measured gain is 35dBi and the beam pattern shows clean side lobe performance as expected from the passive lens element.

8.2.1.2 Radiating element return loss

The graph below shows the measured return loss of the radiating elements across the frequency operation range. The return loss figures at frequencies below 61GHz tend to be lower than -10dB, which means that more then 10% of the power injected into the radiating element is reflected rather than being radiated. Overcoming this problem requires fine tuning of the radiating element match to the driving waveguide impedance.

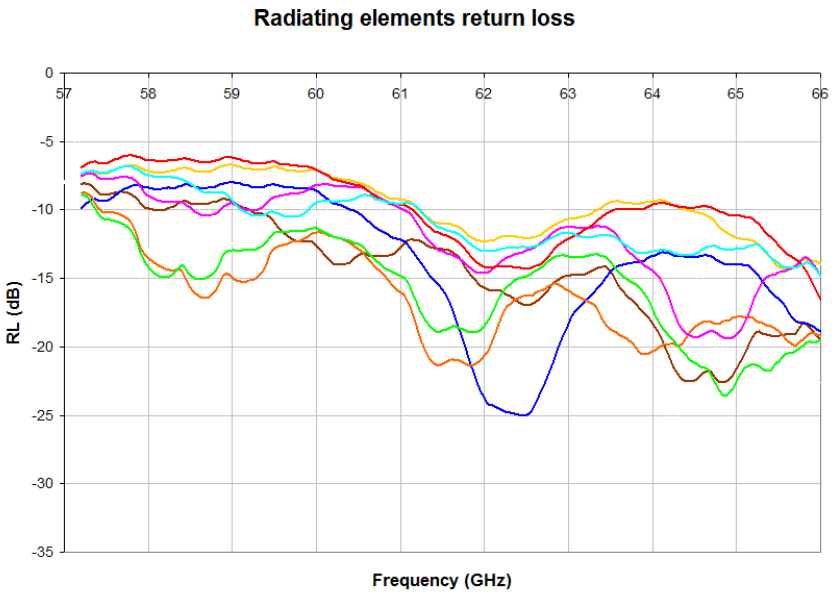

Figure 25: Return-loss performance of the eight radiating elements across frequency

8.2.1.3 Single beam frequency response

The graph below shows the measured gain of a specific beam across the frequency operation range of the antenna. It can be observed that below 61GHz the antenna gain is degraded. This degradation is mostly the result of the poor match at frequency below 61GHz, which causes some of the injected power to be reflected from the radiating element, rather than being radiated. It is believed that once the matching issue is fixed, the antenna gain degradation below 61GHz would be eliminated.

© RAPID5G Consortium

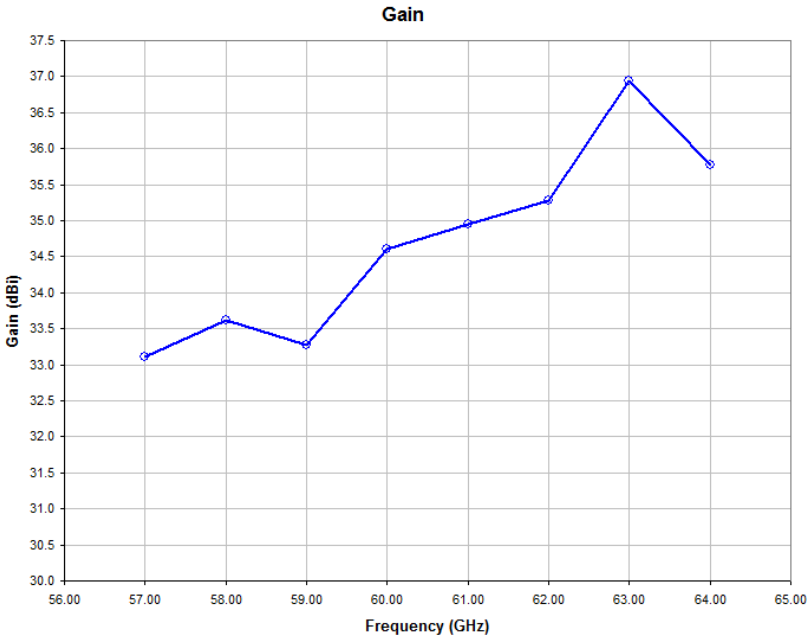

Figure 26: Single beam frequency response

8.2.2 LTCC based construction

8.2.2.1 Individual beam patterns

The LTCC based construction does not enable direct attachment to the radiating elements. Instead, the elements are driven by the RFIC. Variations in the power driven by the RFIC per element exist, as well as variation in the trace length connecting the RFIC to the radiating element. The graphs below show the measured beam patterns resulting from exciting the elements along the horizontal axis. In order to reduce clutter in the graph, each horizontal row is shown separately. Similar to the PCB construction, each element is excited separately and each generates a distinct beam direction. The antenna patterns differ in gain level due to different differences in the driving power as well as differences in the length of trace wire connecting the radiating element to the RFIC port (typical attenuation on the LTCC is ~1dB/cm).

© RAPID5G Consortium

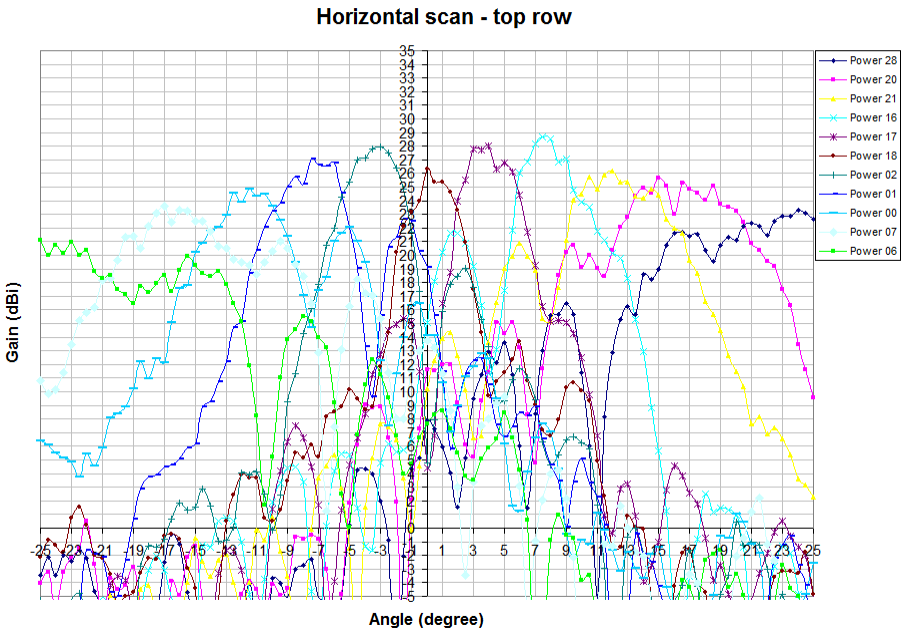

Figure 27: Horizontal scanning beams for top array row

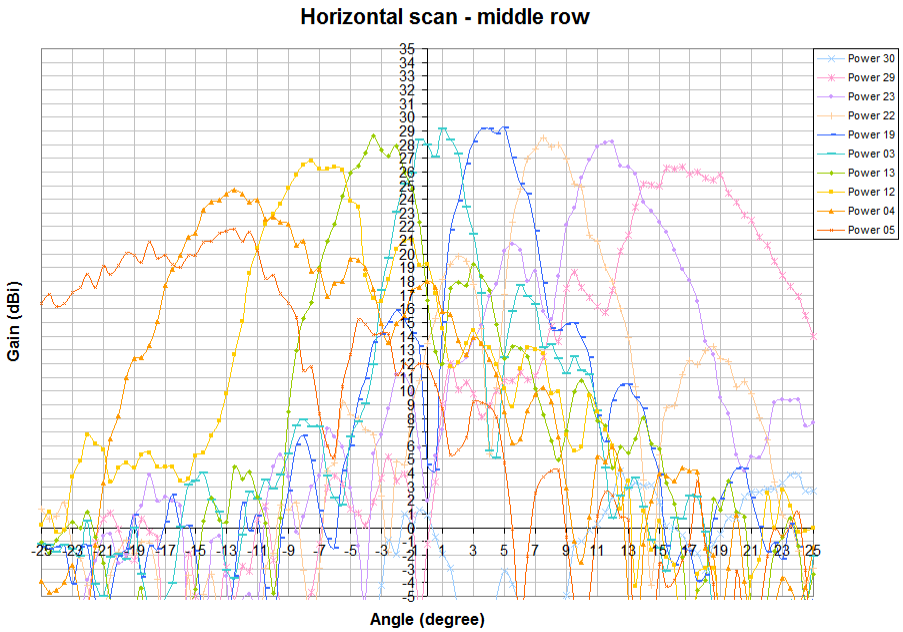

Figure 28: Horizontal scanning beams for middle array row

© RAPID5G Consortium

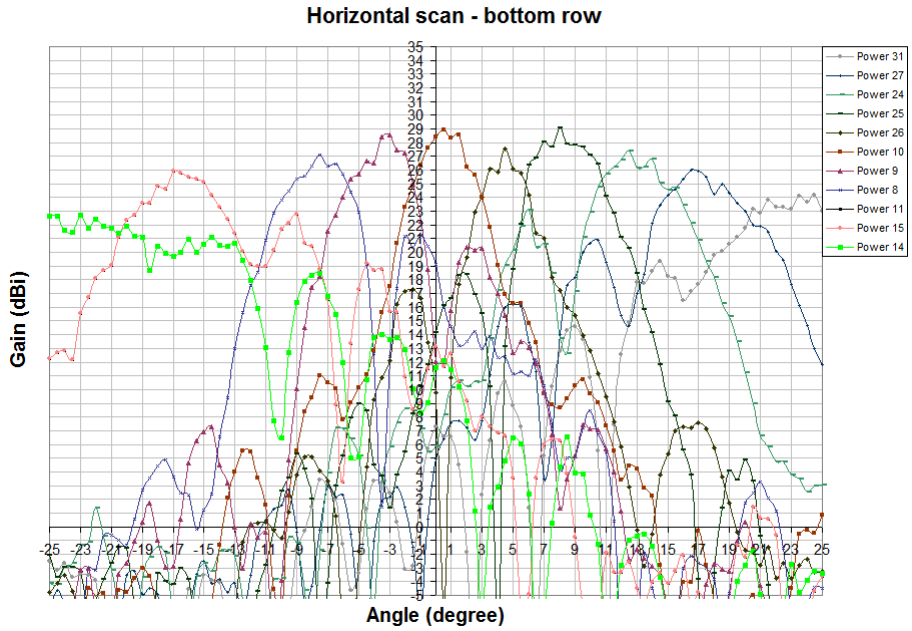

Figure 29: Horizontal scanning beams for bottom array row

From the graphs above it may be concluded that the horizontal scanning range of the antenna would be about ±19° (to the 25dBi point). The top row graph was measured at 5° elevation angle while the bottom row graph was measured at -5° elevation, thus the vertical scanning range would be ±5°. The measured peak gain is 29dBi and the beam pattern shows clean side lobe performance as expected from the passive lens element. It may be noted that the beams farther from the centre suffer from some degradation, which is mostly due to their less efficient illumination of the lens, stemming from the fact that they are far from the centre.

8.3 Theoretical System Evaluation of Switched Beam Antenna Performance (Kent)

The objective of this section is to develop a theoretical estimate the system performance of Siklu's beam-steering system in terms of spectral efficiency (b/s/Hz) and error-vector-magnitude (EVM). The approach adopted was to model a system which can replicate Siklu's beam patterns for the PCB horizontal scan, and subsequently evaluate the performance of a single user located on the angular plane of the beams. Three scenarios have been analyzed.

- Initially, the horizontal beam-patterns and beam gains of Lens A,B,C,H and E (see Figure 23) was matched though modeling and simulation in MATLAB using planar array antennas.
- Subsequently, the performance of beam-switching action for each of these beams was evaluated in terms of spectral efficiency in bits/s/Hz. This was accomplished by locating the user initially on the principal axis of each of the beams, and then sweeping the user though its angular coverage area (in azimuth) as well that of the coverage areas of the other beams treating them as interference and obtaining the Signal to Interference Noise Ratio (SINR). It was assumed that each of the beams has its own dedicated data source.
- Lastly, in order to evaluate the error vector magnitude (EVM), a model was developed in SIMULINK for an OFDM transmit-receive system.

© RAPID5G Consortium

8.3.1 Beam-Pattern Generation, Steering Action and BER Analysis

A beam-pattern with main-lobe gains similar to that of Lens A (35.5dB gain), Lens B (34.5dB), Lens H (32dB), Lens G (35dB), and Lens E (35dB) respectively (see Figure 23), and to estimate the mm-wave spectral efficiency (b/s/Hz). This was implemented using an array steering code which generates an array encoder for a 6x6 planar antenna array with an appropriate phase-shift per every antenna elements for the simultaneous transmission of beams.
The figure below plots the beam-pattern generated in MATLAB.

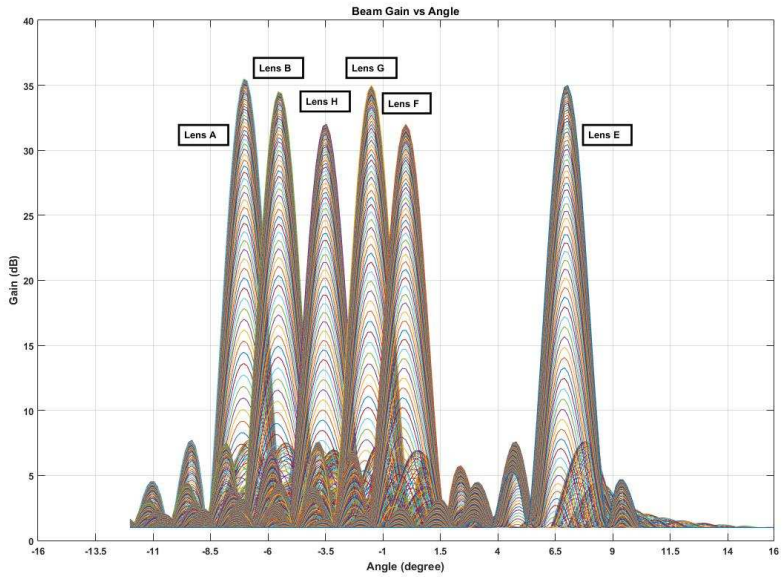

Figure 30: Beam-pattern generation (MATLAB). Planar Antenna Array phase shifts were applied to simulate each of the beam-patterns.

8.3.2 Beam-Switching Action

The scenario is depicted in Figure 39 below:

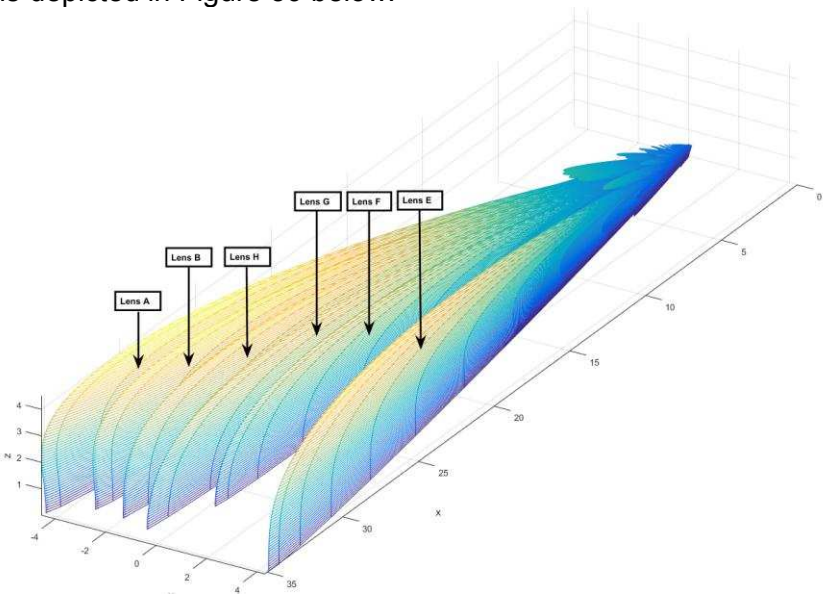

Figure 31: Beam Switching

© RAPID5G Consortium

In Figure 31, six separate beams generated from each of the six radiating elements of the Siklu lens that are modelled in MATLAB, are shown. The angular separations of the beams have been kept identical to that of Siklu's beam-steering PCB set up for horizontal scan.

In the simulation, it is assumed that each of the beams have their own dedicated but same data streams, which can be incorporated in a future variant of Siklu's beam-steering set up by using an RF switching matrix prior to the antenna.

In this model, the angular coverage region of any beam extends from its principal axis to halfway towards the next beam. The performance of the user is evaluated at the each of beam locations in terms of spectral efficiency, as it is swept through the angular plane, with the remaining beams being treated as interference and the corresponding Signal-to Interference-Noise-Ratio (SINR) is obtained. For an N beam system, SINR for the i-th beam is given by:

$$SINR_i = \frac{G_i}{(rvar + G_0 + G_1 + \cdots + G_{i-1} + G_{i+1} + \cdots + G_N)}$$
$$where\ G_i\ is\ the\ gain\ of\ the\ i-th\ beam$$

Figure 32 plots the spectral efficiency (b/s/Hz) for the different angular locations of the user at an, as it moves from the coverage area of one beam to the next. It was benchmarked against the spectral efficiency of a 10dBi antenna which provides coverage over the full angular range, which was compensated for in the SINR. The transmit power level of the 10dBi antenna is equalized to the average of transmit power level of the other beams.

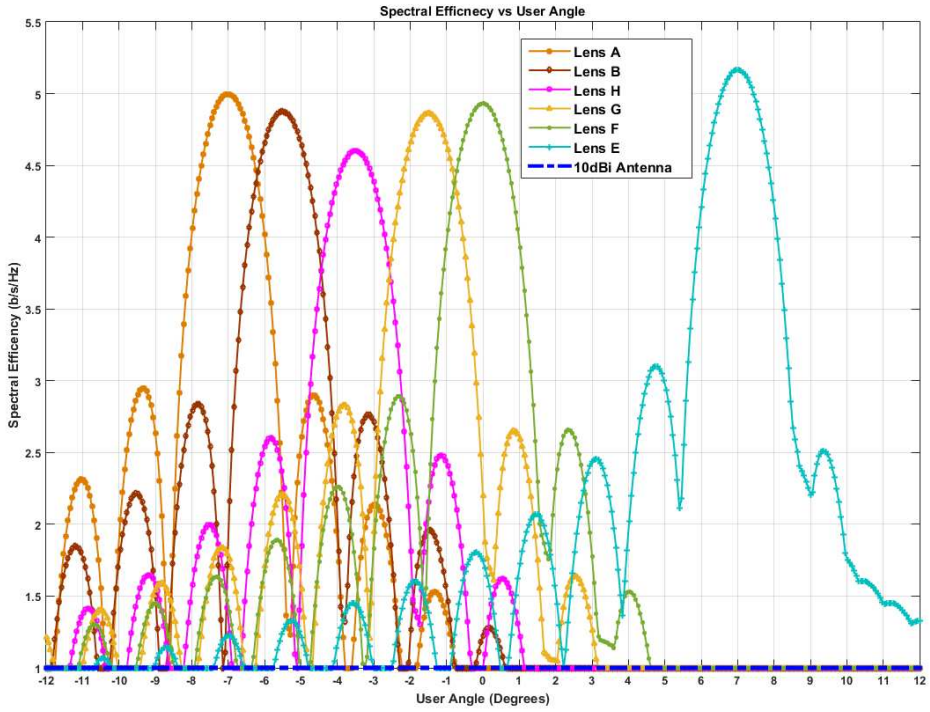

Figure 32: Spectral efficiency (b/s/Hz) vs Angular Sweep of User

© RAPID5G Consortium

In calculating the spectral efficiency of the 64QAM modulated Gray encoded data steam (modulation index, K=6), a chip rate of C=1Gbps at Eb/No=10dB, with channel bandwidth B=1GHz, gives

Signal to noise ratio (SNR) at the user = user_SNR = 10*log10(Eb/No+SINRi) + 10*log10(C/B) + 10log10(K) – FPSL.

FPSL is the free space path loss = 20*log10(d) + 20*log10(fc) + 20*log10(4*pi/c) = ~66dB/m at fc = 60GHz. Path loss distance d = 10m. Spectral Efficiency is then obtained as SE = log2(1+ user_SNR). Each of the beams have the same data stream.

From Figure 32, it can be observed the maximum spectral efficiencies are obtained when the user is within the coverage area of any specific beam. This demonstrates beam switching action in an interference limited scenario.

8.3.3 EVM Estimation in SIMULINK

Furthermore, to estimate the error vector magnitude (EVM), a beam-steering system that generates the same beam gain as Siklu's antenna (Lens E, Horizontal PCB scan) was developed in SIMULINK.

An OFDM frame with pilots was generated to model a realistic system. The parameters for the OFDM frame are:

- IFFT length=2048; CP length=512; QAM level=64; Data Carriers' Symbol Rate=3.143310546875E+07; No pilots=16; Pilot subcarrier indices in an OFDM frame=[183:108:1803];

Figure 33 shows the set-up of the SIMULINK model.

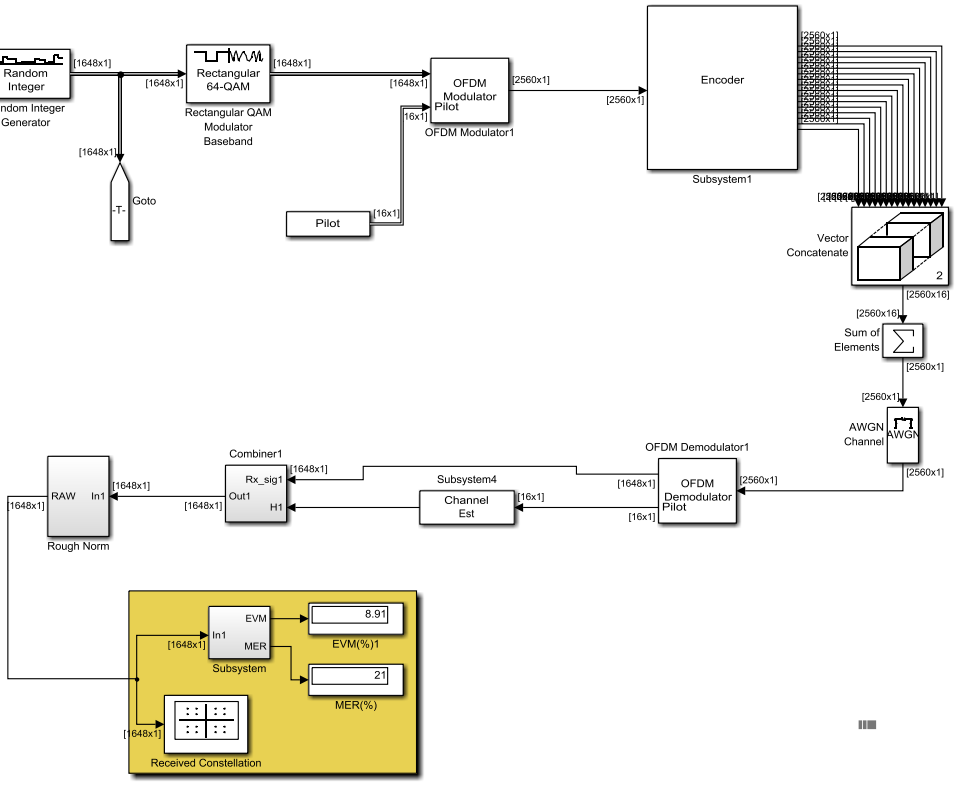

Figure 33: Array-steering set up in SIMULINK

© RAPID5G Consortium

The elements in the set-up shown above are as follows:

- Random Integer Generator: Generate random uniformly distributed integers in the range [0, M-1], where M is the M-ary number.
- Goto: Send signals to and from blocks that have the specified tag.
- Rectangular QAM Modulator Baseband: Modulate the input signal using the rectangular quadrature amplitude modulation method. This block accepts a scalar or column vector input signal.
- OFDM Modulator: Apply OFDM modulation to the input signal. Enable pilot signal input to assign it into designated subcarriers prior to modulation.
- Encoder: Linear encoder generated based on the array-steering matrix explained previously
- Vector Concatenate: Concatenate input signals of the same data type to create a contiguous output signal. Select vector or multidimensional array mode.
- Sum of Elements: Add or subtract inputs.
- Channel AWGN: Add white Gaussian noise to the input signal. The input signal can be real or complex. This block supports multichannel processing.
- OFDM Demodulator: Apply OFDM demodulation to the input signal. Enable pilot signal output to separate it from the data signal after demodulation.
- Channel Est: Estimate the channel coefficients based on received OFDM pilots

For the set-up of Figure 33, the array encoding has been implemented at the baseband upon the modulated OFDM symbols. For an SNR of 10dB, the EVM generated in SIMULINK for this array was 8.91%.

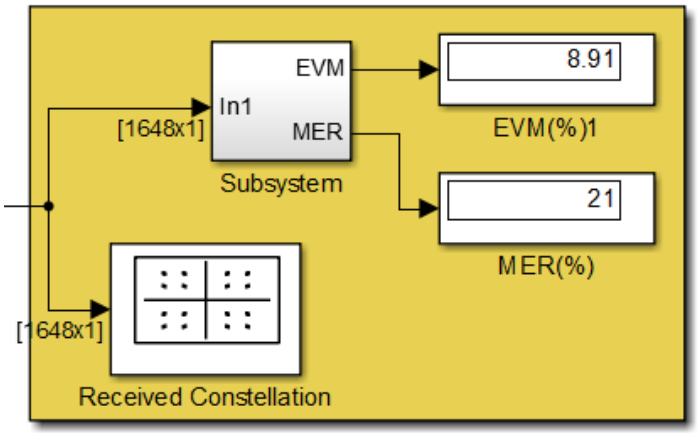

Figure 34: Error Vector Magnitude (EVM)

For future work, the SIMULINK model will be enhanced for implementing array encoding in the RF domain.

8.4 Electro-optical beam-steering antenna (Osaka)

The electro-optical antenna will be reported in detail in D322. However, preliminary results are already provided here to give a comprehensive overview of the chosen technology.
A preliminary experiment for SDM channel discrimination was done by using an experimental setup for bidirectional light-wave input and output shown below. Two laser sources and optical circulators were used. One of the light-waves was input to a waveguide from the left side, and another was input to the same waveguide form the right side. The input and output optical signals were separated by the circulators, and the spectra of the output signals were measured by optical spectrum analyzers.

© RAPID5G Consortium

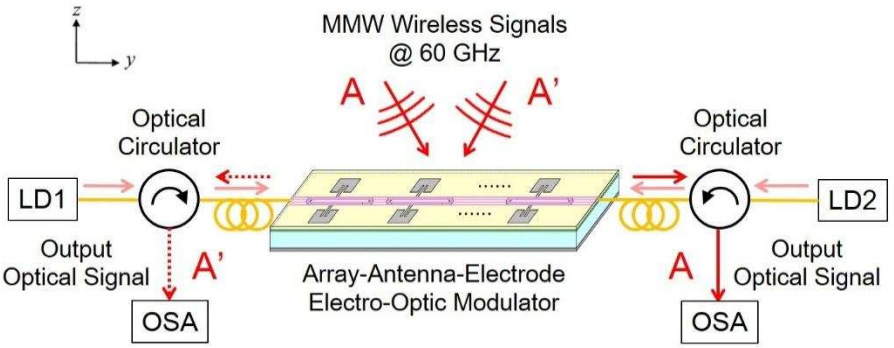

Figure 35: Experimental setup for SDM channel discrimination

The experimental result is shown below. The wireless signal of channel A was obtained by injecting light-wave from the left side. On the other hand, the channel A' signal was also obtained by propagating the light-wave along the opposite direction. From these results, the discrimination of 2 SDM channels in a single waveguide was confirmed successfully.

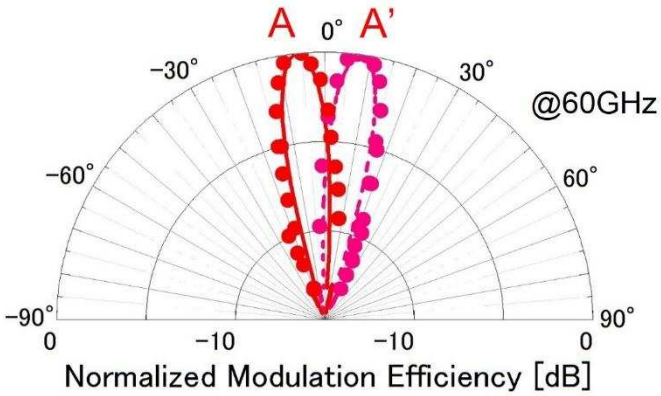

Figure 36: Experimental result of SDM channel discrimination by bidirectional optical input

© RAPID5G Consortium

9 Concluding remarks

Several different methods and constructions of 1D and 2D beam steering antenna have been reported in this document. The methods and constructions are adapted to the use case requirements and employ different implementations; some utilize frequency scanning, other use various lens and others use EO to mm-wave conversion. These techniques result in different gain and steering capabilities. All antennas have been characterized in their frequency band of operation extending from 57 GHz to 64 GHz.

The travelling-wave antenna was intended for a low-cost 1D beam-steering antenna using carrier frequency scanning. The fabricated antennas provide a gain of about 12 dBi, 1D beam steering over about 20° within the 57-64 GHz frequency range of interest and H-plane and E-plane 3 dB beam width of 6° and 60°. Thus the antennas are expected to fulfil the requirements for the hot spot use case by enabling wireless transmission of up to at least 2.5 Gbit/s over a few meters.

The beam switching LTCC based construction which was intended as a broadband steering antenna meets the gain target required in the system specification. The wide lens was designed for 45° scanning overage, so two such devices would be able to realize a beam steering coverage of 90°. The actual measured scanning coverage falls slightly short of this figure with about 38° of scanning coverage, indicating that perhaps the radiating elements should have been spaced with a slightly higher distance in order to achieve 45° scanning coverage.

© RAPID5G Consortium

10 References

[1] RAPID deliverable D211, "System Architectures for Dense User Access Network Scenario"

[2] RAPID deliverable D421, " Heterogeneous radio resource management functions"

[3] RAPID deliverable D221, "Subsystem and component specifications"

[4] Fanyi Meng, Chirn Chye Boon, Shanshan Xu, Kaixue Ma, Kiat Seng Yeo, "Millimeter-wave IC design techniques for beam-forming applications", IEEE International Workshop on Electromagnetics: Applications and Student Innovation Competition (iWEM), 2016

[5] Buttgenbach, T. H., “Improved solution for integrated array optics in quasi-optical mm and submm receivers: The hybrid antenna,” IEEE Trans. Microw. Theory Tech., Vol. 41, No. 10, Oct. 1993, 1750–1761

[6] Hirokawa J., “Analysis and fabrication of millimeter-wave slotted waveguide array antennas”, Electromagnetic Theory (EMTS), 2010 URSI International Symposium on

[7] Lim S., Caloz C., Itoh T., “Electronically Scanned Composite Right/Left Handed Microstrip Leaky-Wave Antenna”, IEEE MICROWAVE AND WIRELESS COMPONENTS LETTERS, VOL. 14, NO. 6, JUNE 2004

[8] Dadgarpour, A., B. Zarghooni, B. S. Virdee, and T. A. Denidni, “Beam-deflection using gradient refractive-index media for 60-GHz nnd-Fire antenna,” IEEE Trans. Antennas Propagation, Vol. 63, No. 8, Aug. 2015

[9] M. Sterner, D. Chicherin, A.V. Räisenen, G. Stemme, J. Oberhammer, "RF MEMS HIGH-IMPEDANCE TUNEABLE METAMATERIALS FOR MILLIMETER-WAVE BEAM STEERING", Proceedings of the IEEE International Conference on Micro Electro Mechanical Systems (MEMS), March 2009

[10] M. Fakharzadeh, M. R. Nezhad-Ahmadi, B. Biglarbegian, J. Ahmadi-Shokouh, S. Safavi-Naeini, "CMOS Phased Array Transceiver Technology for 60 GHz Wireless Applications", IEEE TRANSACTIONS ON ANTENNAS AND PROPAGATION, VOL. 58, NO. 4, APRIL 2010

[11] A. Tamminen, J. Ala-Laurinaho, S. Mäkelä, A. V. Räisänen, D. Gomes Martins, J. Häkli, P. Koivisto, P. Rantakari, J. Säily, R. Tuovinen, A. Luukanen " Millimeter-wave reflectarray for beam-steering applications", 7th European Microwave Integrated Circuits Conference (EuMIC), 2012

[12] M. Y. Ismail, M. Inam, "Design of Liquid Crystal Based Tunable Reflectarray Antenna Using Slot Embedded Patch Element Configurations", World Academy of Science, Engineering and Technology International Journal of Electrical, Computer, Energetic, Electronic and Communication Engineering Vol.8, No.10, 2014

© RAPID5G Consortium